URock 2023a: An open source GIS-based wind model for complex urban settings

Jérémy Bernard[1,2,3], Fredrik Lindberg[1], and Sandro Oswald[4]

[1]University of Gothenburg, Department of Earth Sciences, Sweden
[2]University of Savoie Mont-Blanc, LOCIE, UMR 5271, France
[3]CNRS, Lab-STICC, UMR 6285, Vannes, France
[4]Institute of Meteorology, University of Natural Resources and Life Science (BOKU), Vienna, Austria

Correspondence: Jérémy Bernard (jeremy.bernard@zaclys.net)

Abstract. URock 2023a is an open source diagnostic model dedicated to wind field calculation in urban setting. It is based on a quick method initially proposed by Röckle and already implemented in the proprietary software QUIC-URB. First, the model method is described as well as its implementation in the free and open source geographic information system called QGIS. Then it is evaluated against wind tunnel measurements and QUIC-URB simulations for four different building ~~settings~~ layouts plus one case with an isolated tree. The correlation between URock and QUIC-URB is high and URock reproduces quite well the spatial ~~variations~~ variation of the wind speed observed in the wind tunnel experiments~~. Sources of improvementsare highlighted~~, even in complex settings. However, sources of improvements, which are applicable both for URock and QUIC-URB~~. URock~~, are highlighted. URock and QUIC-URB overestimate the wind speed downstream the upwind edges of wide buildings and also downstream isolated tree crowns. URock 2023a is available via the Urban Multiscale Environment Predictor (UMEP), a city-based climate service tool designed for researchers and service providers presented as a plugin for QGIS. The model, data and scripts used to write this manuscript can be freely accessed at https://zenodo.org/record/7681245.

1 Introduction

Due to climate change, thermal comfort is ~~getting~~ becoming an important topic in the urban planning process. An outdoor space should be comfortable during summer time~~but also remains~~, but should also remain comfortable during winter time. Shortwave and longwave radiation, wind speed, air temperature and relative humidity are the main meteorological variables that impact the human heat balance. Radiation and wind speed are the variables ~~the most spatially sensitive to a small variation of an~~ spatially most sensitive to small variations in the urban configuration: a new building will create shadow and also, in most cases, decrease the wind downstream. This will affect the outdoor thermal comfort and the weather conditions at the buildings boundaries, which may also impact indoor thermal comfort. Thus, there is a need for easy to use tools to calculate the level of radiation received by surfaces ~~in an urban setting~~ and also the spatial variations of the wind in an urban setting. Several tools already exist to achieve this work such as ~~Envi-met~~ ENVI-met (Huttner and Bruse, 2009; Bruse, 2004), SkyHelios (Matzarakis et al., 2021), ~~Solene-microclimate (Morille et al., 2015; Musy et al., 2021) or~~ SOLENE-microclimate (Morille et al., 2015; Musy et al., 2021) or Eddy3D (Kastner and Dogan, 2022). However, these tools are proprietary soft-

wares (or not publicly available ~~concerning Solene-microclimate~~like SOLENE-microclimate) making their use ~~difficult for community development purpose~~and community development difficult. PALM is a 3D, CDF modelling system that can be used to predict the wind in urban area using the PALM-4U components (Maronga et al., 2020). It is designed to model complex physical phenomenons and is thus not ~~dedicated~~ designed to run large areas on a personal computer. ~~More recently~~Recently, an open source model (QES-Winds), based on the QUIC-URB~~one~~ , has been developped by Bozorgmehr et al. (2021). Urban Multi-scale Environmental Predictor (UMEP) is a climate service tool that can be used for a wide variety of applications including thermal comfort (Lindberg et al., 2018). It is developped as a plugin available ~~in~~ to the free and open source QGIS software. This integration facilitates the user interaction with spatial information to determine model parameters, and to edit, map and visualise ~~inputs and~~ the inputs and the results. For this reason, this cross-platform, free and open source tool is well suited for both researcher and practitioners within the field or urban climatology. However, it does not have any model dedicated to wind calculation yet. This article presents the URock model, which has been recently developped and ~~added~~ integrated into UMEP.

The ~~requirement specifications were to have~~ aim was to develop a relatively fast and accurate model ~~, simple of use and resulting in~~ which is simple to use and able to generate a wind field ~~that can be used for~~ usable by both indoor and outdoor applications (comfort and pollution). Many options were considered: prognostic models, statistical models and diagnostic models. ~~The first consists~~ Prognostic models consist in solving the Navier-Stokes equations through numerical methods. While this is probably the most accurate method, it is also the slowest and ~~needs~~ requires a certain degree of expertise for a user to ~~have~~ obtain relevant results (Tominaga et al., 2008). ~~The second consists~~ Statistical models consist in using relationships that have been established between observed or simulated wind speed fields and a given set of explanatory variables such as distance to a wall or a tree, sky view factor, etc. (Calzolari and Liu, 2021; Johansson et al., 2016). However, these relations are only valid for cases where the urban setting remains ~~quite close from~~ close to the one(s) used to create the model ~~. It can then be quite inaccurate in some specific urban settings~~ (Johansson et al., 2016). Moreover, atmospheric pollution and building applications ~~need~~ requires a three dimensional field and ~~for~~ the three components of the wind~~, rendering the statistical modelling quite inappropriate~~. These requirements render the statistical model unsuitable for these applications. The last option, called diagnostic model, is a good compromise between the ~~two first~~prognostic and statistical models. It is a two steps approach~~: in~~ . In the first step, the wind speed and wind direction are initialized in several zones around wind obstacles. The location and size of the zones, as well as the values used for wind speed and wind direction, are derived from wind tunnel observations. The second step consists ~~in~~ of balancing the air flow while minimizing the modifications of the initial wind field. Initially, this method was implemented at larger scale (~~buildings were not considered~~no building consideration) to take into account the effect of terrain ~~elevation~~ on the wind (Sherman, 1978; Ratto et al., 1994). At this scale, the initialization stage is ~~not based on empirical laws deduced from wind tunnel experiments but~~ performed using wind observations: the wind speed is initialized in locations where wind observations are available. ~~The~~ Using this method, the resulting wind field ~~using this method is in quite~~ is in good agreement with observations or wind fields derived from prognostic models (Wellens et al., 1970). Röckle (1990) was the first to propose a ~~quite~~ detailed set of empirical laws to initialize the wind speed around buildings. ~~At~~ To our knowledge, the first software implementation of its work, called QUIC-URB, has been developped by Pardyjak and Brown (2003) and

is available on request as a proprietary software. Several modifications have been performed to improve the model accuracy: some of the empirical laws proposed by Röckle (1990) have been modified and new zones have also been created (Bagal et al., 2004; Pol et al., 2006; Nelson et al., 2009). The QUIC software is initially dedicated to pollution dispersion~~but~~. However, the 3D wind field generated by QUIC-URB can also be used for outdoor thermal comfort applications (Girard et al., 2018) and for building energy or building thermal comfort applications thanks to a pressure solver model (Brown et al., 2009b). Recently, Fröhlich (2016) and Fröhlich and Matzarakis (2018) have implemented in SkyHelios a diagnostic model, which is also based on the Röckle (1990) methodology and the QUIC-URB improvements. However, as previously highlighted, these models are not ~~available as free and open sourcecode~~free or open source. Moreover, the methodology used for the initialization step is not fully described.

This article presents the detailed methodology used by the free and open source diagnostic model URock, which has been implemented in UMEP (Sect. 2). Its implementation in UMEP is described Sect. 3. Several wind tunnel experiment data are freely available thanks to the Architectural Institute of Japan (AIJ). These data are used to verify that URock reproduces well the wind field generated by QUIC-URB and also to investigate ~~what are~~ the main modifications that could be performed in these ~~current~~ diagnostic models to improve their accuracy (Sect. 4).

2 Model description

URock can ~~be used to~~ calculate the 3D wind field of an urban area using information about the wind (at least speed and direction at a given height) and ~~geographical data describing~~ the area of interest (~~building and vegetation~~ the footprint and height ~~). Two main stagesare used~~of building and vegetation). The calculation consists of two main stages: wind field initialization and wind field balance.

The wind field is initialized according to empirical laws drawn from wind tunnel experiments. ~~As~~ Because QUIC-URB is ~~nowadays~~ the most validated diagnostic model, all zones and their corresponding empirical laws used in URock are the ones also ~~used~~ defined in QUIC-URB. In URock, nine different zones are identified around buildings and within vegetation:

- Six zones belong to isolated buildings (Fig. 1a),
- A single zone (the so-called street-canyon) is created between two ~~buildings close to each other~~ adjacent buildings (Fig. 1b).
- Two distinct zones are created within vegetation depending of their proximity ~~with~~ to buildings (Fig. 1c).

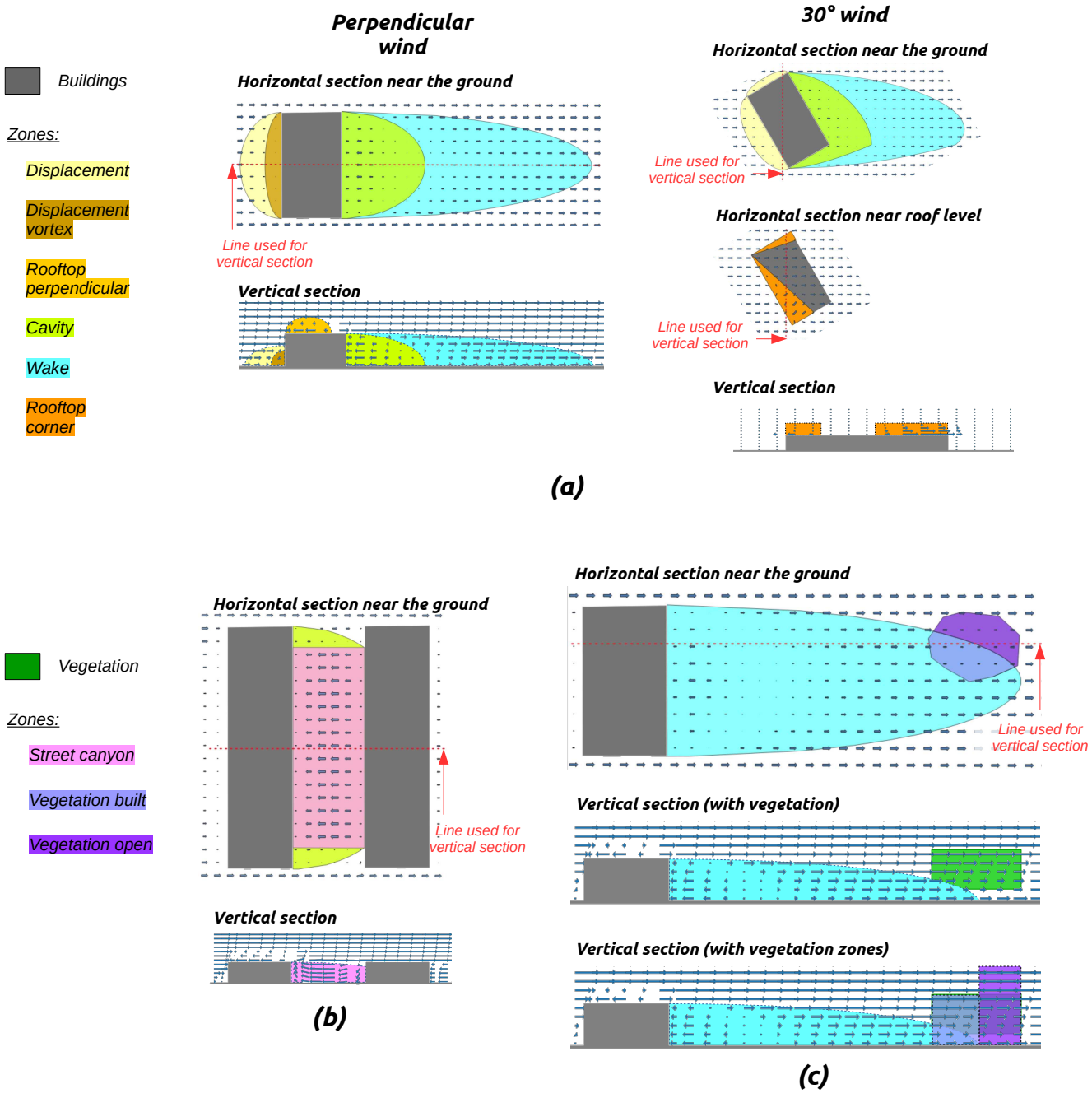

Figure 1. Illustration of the nine zones used in URock to initialize the wind field: (a) zones created by isolated building, (b) zones created between ~~nearby~~ adjacent buildings and (c) zones created within vegetation.

The size of each of these zones is calculated from obstacle properties (such as height, length and width for building or attenuation capacity for the vegetation). The wind speed and wind direction depends on the zone type and location within the zone (distance to the wall, to the ground or the end of the zone). More informations about each of the zones will be given in Sect. 2.3.2 (building zone size), 2.3.3 (vegetation zone size) and 2.3.4 (building and vegetation wind factors).

The wind field is then numerically balanced in order to make it physically relevant with the constraint to minimize the differences with the initial wind field.

The algorithm used in URock is based on the following procedure (illustrated in Fig. 2):

1. Create URock geometries: the input geographical data is initialized into the format needed for the URock calculations,
2. ~~Effect~~ Derive the effect of all obstacles on the wind: some morphometric properties of the study area are calculated and can be used to set a mean wind profile,
3. ~~Effect~~ Derive the effect of individual obstacles on the wind: each obstacle is considered individually to set the initial wind factor near buildings and within vegetation,
4. Calculates wind speed: the 3D wind speed components are initialized for each cell of the ~~sketch~~ domain and then used in the numerical solver to ~~get~~ obtain the final balanced wind field.

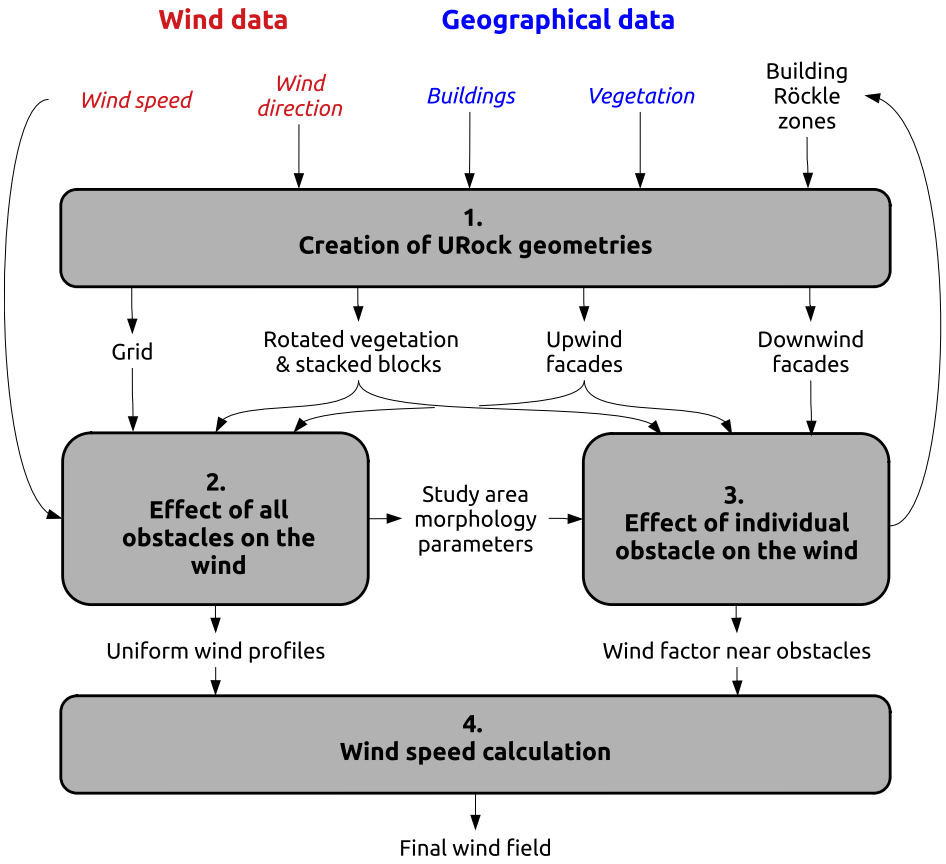

Figure 2. Overall methodology used by the URock model

Each step of this procedure will be described in the following subsections.

2.1 Creation of URock geometries

This step is dedicated to *(i)* the transformation of standard input vector geometries into a format that ~~will~~ facilitates the wind speed initialization and ~~also to create the~~ *(ii)* the creation of the grid used for numerical solving. The following processes are used (Fig. 3). First, individual buildings are converted to stacked blocks. Then, the entire ~~sketch~~ domain (buildings and vegetation) is rotated to ~~always~~ have the wind coming from the North. Last, a 3D grid of rectangular-based cells is created and the facades ~~being~~ located upwind as well as those ~~being~~ located downwind are identified.

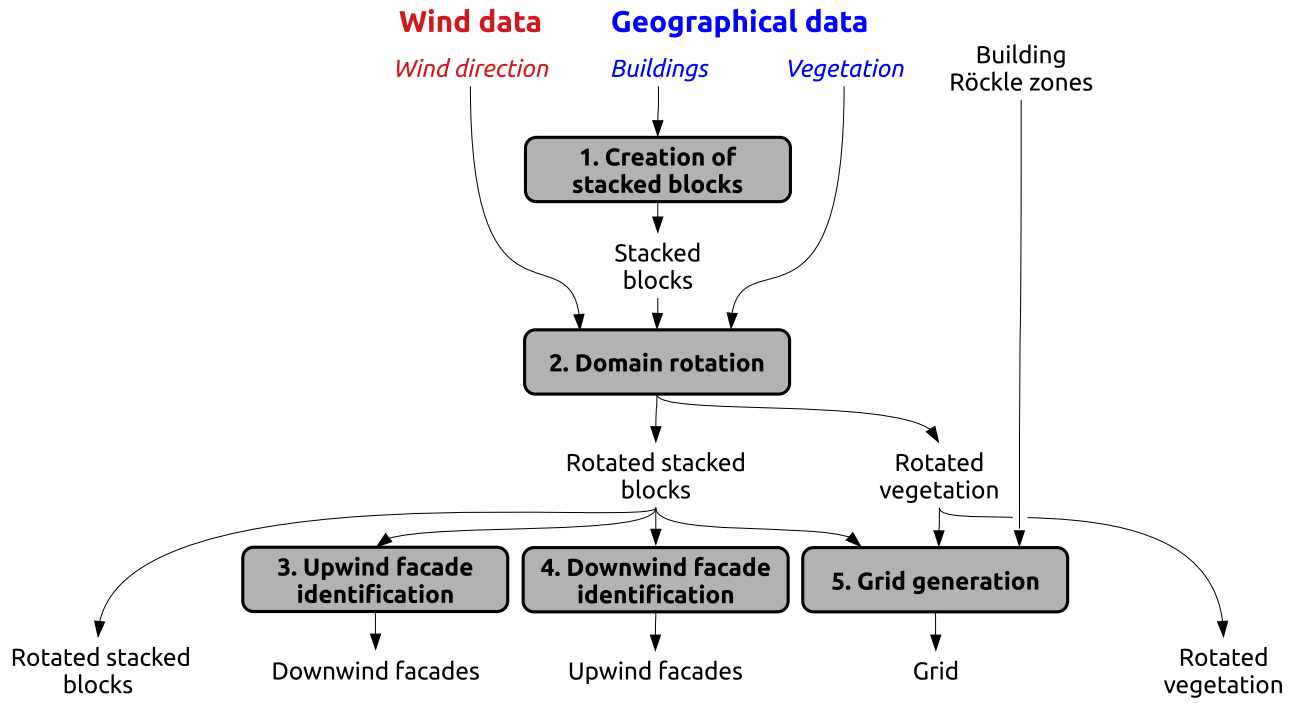

Figure 3. Procedure used to create the URock geometries

2.1.1 Creation of stacked blocks

Buildings may have an oversampled number of points, which may result in a considerable amount of Röckle zones (some of the zones are created for each unique segments) and thus results in low computation efficiency. ~~To~~ In order to avoid such issue, building geometries are first simplified ~~removing useless~~ by removing unnecessary points[1].

The size of a Röckle zone depends on the size of the obstacle. In URock, buildings touching each other but having a different height are transformed into vertically stacked blocks as shown in Fig. 4 ~~(~~— method also used in QUIC-URB~~)~~. A preliminary task is to merge buildings touching each other or being within a given distance to each other. A buffer is created around each building[2] and the footprints touching each other are spatially unioned. Then, we round building height values ~~and we~~ to the nearest integer and create as many stacked blocks as there are isolated blocks of same height.

[1]This is done using the H2GIS ST_Simplify function (http://www.h2gis.org/docs/dev/ST_Simplify/) with distance = GEOMETRY_SIMPLIFICATION_DISTANCE (default 0.25 m)

[2]This is done using the H2GIS ST_BUFFER function (http://www.h2gis.org/docs/dev/ST_Buffer/) with bufferSize = SNAPPING_TOLERANCE (default 0.3 m) and bufferStyle='join=mitre'

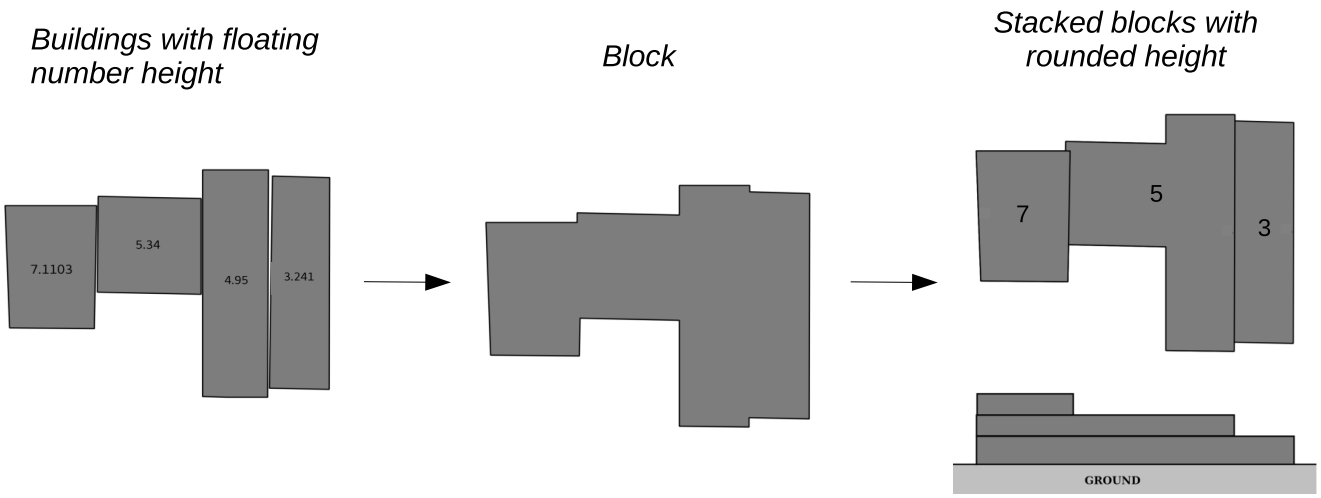

Figure 4. Method used to convert buildings to stacked blocks

2.1.2 ~~Sketch~~ Domain rotation

All obstacles are rotated in order to have the wind coming downward to simplify the equations used in the initialization step. The rotation center is defined as the top right corner of the smallest bounding box containing all obstacles.

2.1.3 Upwind facades identification

Each facade (defined as individual segment belonging to a given stacked block) facing the wind is identified in order to apply the displacement zone scheme. This scheme affects from the bottom of the facade and up to 60% of the facade height. Thus, first several facades belonging to (or nearby) a same vertical plan are merged in order to avoid unexpected displacement zone scheme ~~such as illustrated~~ as illustrated in Fig. 5a[3]. The facade base height $H_{FB_{i+1}}$ (H_{FB_1} in Fig. 5b) of the upper stacked block is then set to the base height of the bottom stacked block.

[3] a facade from an upper stacked block is snapped to the facade of the lowest stacked block if sufficiently close using the function ST_SNAP (http://www.h2gis.org/docs/dev/ST_Snap/) with a snapTolerance = SNAPPING_TOLERANCE (default 0.25 m)

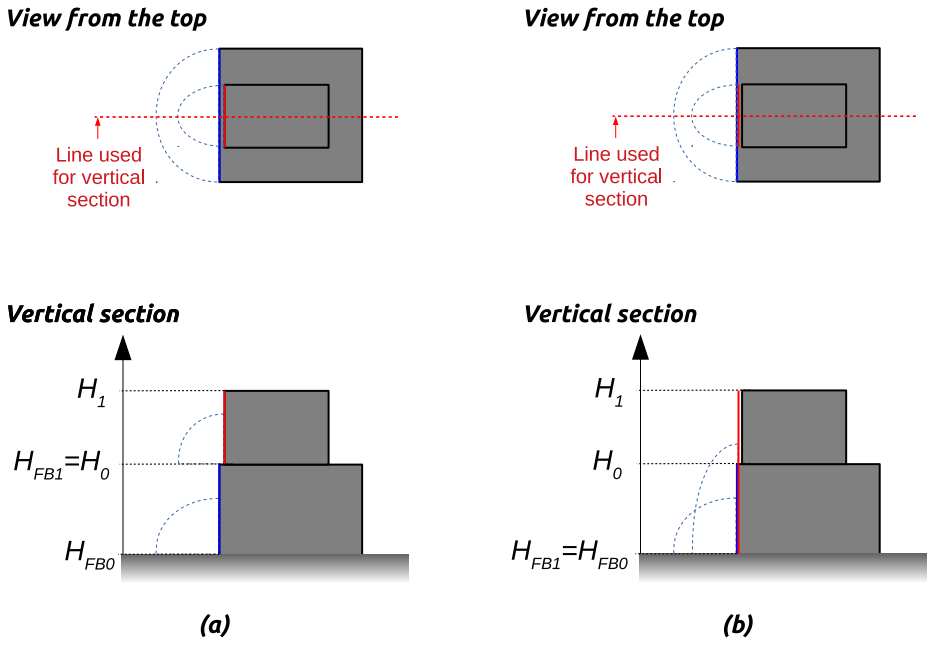

Figure 5. Facade base height and displacement zone of an upper stacked block if the facade is (a) outside or (b) within the snapping tolerance

2.1.4 Downwind facades identification

Each downwind facade (defined as linestring - multisegments connected to each other) is identified in order to apply the cavity and wake zone schemes. Wake zones are defined from the ground while cavity zones starts at cavity base height (H_{CB}). In URock, the cavity zone of a stacked block *i* may alter the cavity zone of the stacked block *i-1* located below up to its cavity base height (H_{CB_i} - Fig. 6). This property is defined Eq. 1 ~~((Brown et al., 2009a))~~(Brown et al., 2009a).

$$H_{CB_i} = H_{B_i} - \frac{L_i}{L_{i-1}} \cdot (H_{i-1} - H_{B_{i-1}}) \tag{1}$$

where H_{B_i} is the base height of stacked block *i* above ground level~~,~~; $H_{B_{i-1}}$ is the base height of stacked block *i-1* above ground level~~,~~; H_{i-1} is the top height of stacked block *i-1* above ground level~~,~~; L_i is the cross wind width of stacked block *i*~~,~~; L_{i-1} is the cross wind width of stacked block *i-1*.

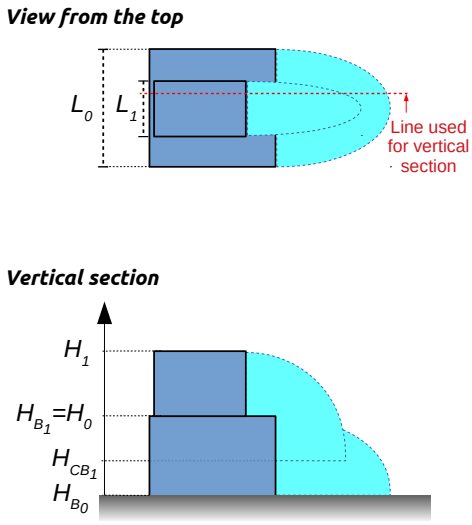

Figure 6. Cavity base zone extension for downwind facades of an upper stacked block

2.1.5 Grid generation

The grid of rectangular-based cells is created according to a horizontal and a vertical resolution set by the user. The size of the grid is defined as an extend distance beyond the built Röckle zones and vegetation boundaries (Fig. 7). By default, the values for the ~~extends~~ extensions are 60 m, 40 m and 20 m respectively for along-wind, cross-wind and vertical axis[4].

[4]these values can be modified in the code by the user using respectively ALONG_WIND_ZONE_EXTEND, CROSS_WIND_ZONE_EXTEND and VERTICAL_EXTEND variables

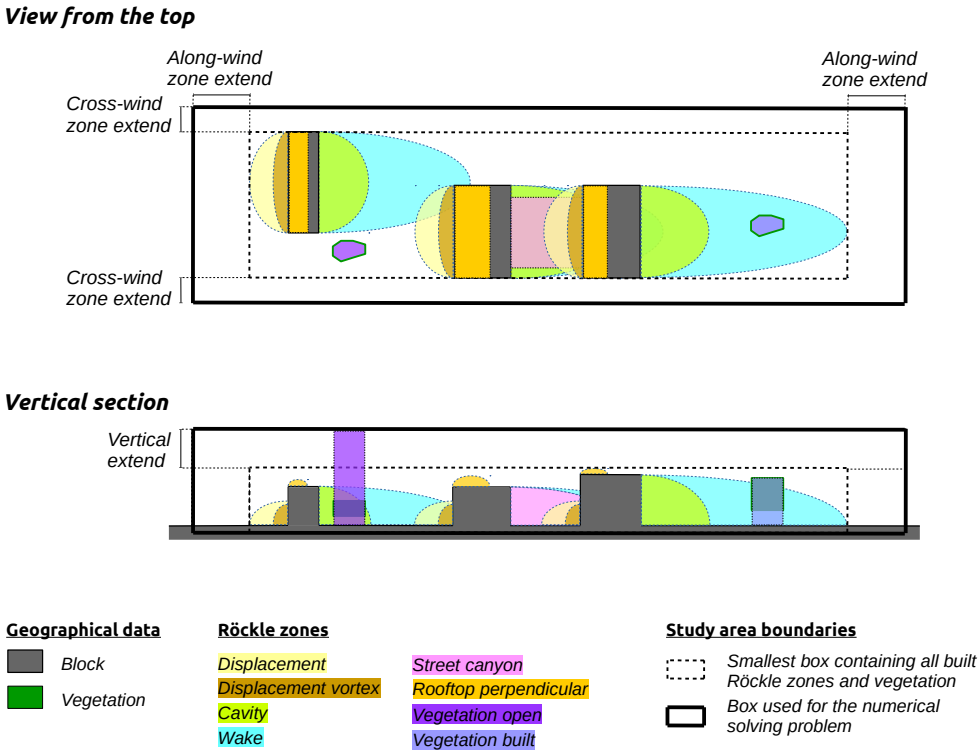

Figure 7. Domain size definition according to along-wind zone~~extend~~, cross-wind zone ~~extend~~ and vertical ~~extend~~extensions

2.2 Effect of all obstacles on the wind

The vertical wind profile is initialized considering mean roughness properties of the study area (Fig. 8).

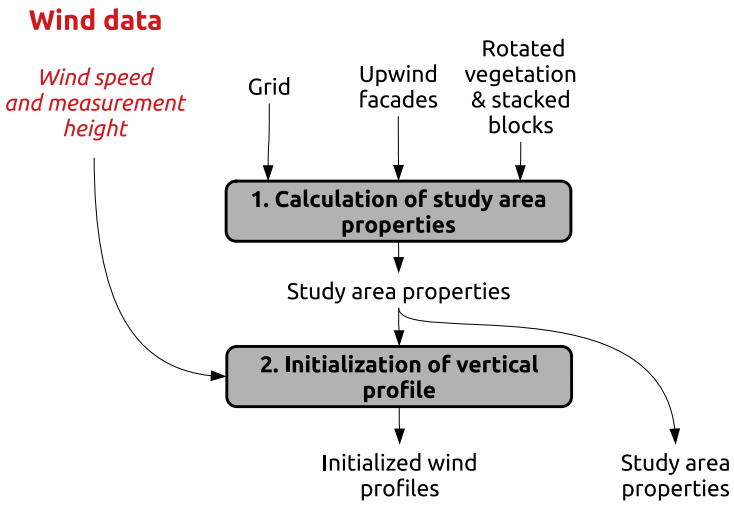

Figure 8. Procedure used takes into account the effect of all obstacles on the wind field

2.2.1 Calculation of study area properties

The roughness height (z_0) and displacement length (d) are both calculated as a unique value characterizing the entire study area. The method described by Hanna and Britter (2002) is used. First, the normalized frontal area (λ_f) is calculated as the ratio between the projected frontal area of obstacle facing the wind (A_f) and the horizontal area of the smallest rectangle containing all buildings and vegetation (A_T). Then z_0 and d are calculating based on the area-weighted geometric mean obstacle height (H_r) and the ~~(~~λ_f ~~)~~ value. Note that the equations ~~differ upon (~~vary as a function of λ_f ~~) values~~ (Tab. 1).

Table 1. Displacement length and roughness height equations depending on the normalized frontal area value. ~~*Note that Hanna et Britter specified that these relations are valid for an upper Hr limit of about 20 m, thus it may lead to higher error if applied to neighborhoods such as skyscrapers.*~~*Note that Hanna and Britter (2002) specified that these relations are valid for an upper Hr limit of about 20 m, thus it may lead to higher error if applied to neighborhoods consisting of skyscrapers.*

Condition	Displacement length~~d (m)~~ , d [m]	Roughness height, z0 ~~(m)~~ [m]
$\lambda_f <= 0.05$	$d = 3 \cdot \lambda_f \cdot H_r$	$z_0 = \lambda_f \cdot H_r$
$0.05 <= \lambda_f < 0.15$	$d = 0.15 + 5.5 \cdot (\lambda_f - 0.05)$	$z_0 = \lambda_f \cdot H_r$
$0.15 <= \lambda_f < 1$	$d = 0.7 + 0.35 \cdot (\lambda_f - 0.15)$	$z_0 = 0.15 \cdot H_r$
$1 <= \lambda_f$	d = 1	$z_0 = 0.15 \cdot H_r$

2.2.2 Initialization of vertical profile

In this URock version, the vertical wind speed profile is set homogeneously on the entire calculation domain. Three possible choices are currently available to set the vertical profile using:

1. ~~a~~ A power-law~~such~~ , as defined by Pardyjak and Brown (2003) (Eq. 2),

2. ~~an urban profile defined as an exponential increase within the canopy (Cionco, 1972) and logarithmic increase above the canopy (Eq. 3),~~

3. ~~a user defined profile.~~

$$V(z) = V_{ref} \cdot (\frac{z}{z_{ref}})^p \tag{2}$$

where $V(z)$ is the wind speed at height z above ground level~~,~~ ; V_{ref} is the reference wind speed observed (or modeled) at the reference height~~,~~ ; z_{ref} is the height above ground level of the reference wind speed~~,~~ ; $p = 0.12 \cdot z_0 + 0.18$ is the exponent of the power-law where z_0 is the roughness height of the study area (Matzarakis and Endler, 2009).

4. An urban profile, defined as an exponential increase within the canopy (Cionco, 1972) and logarithmic increase above the canopy (Eq. 3),

$$V(z) = \begin{cases} V_{ref} \cdot exp(a \cdot (\frac{z}{H_r} - 1)) & \text{if } z < H_r \\ V_{ref} \cdot \frac{log(\frac{z-d}{z_0})}{log z_{ref} z_0} & \text{otherwise} \end{cases} \tag{3}$$

where $a = 9.6 \cdot \lambda_f$ is the attenuation coefficient (Macdonald, 2000), λ_f is the normalized frontal area, H_r is the area-weighted geometric mean height of all obstacles, z_0 is the roughness height, d is the displacement length (Tab. 1) ~~.~~

5. A user defined profile.

The ~~two first solutions only~~ first two solutions need a reference height~~and~~ , the corresponding wind speed and information about the roughness of the area as input while the ~~second~~ third solution needs to have wind speed observed / modeled at several height in the atmosphere.

2.3 Effect of individual obstacles on the wind

Obstacles locally alter the wind field: wind direction or/and wind speed may be modified within vegetation and around buildings. The Röckle approach is applied to set an initial wind factor to those locations using seven building schemes and two vegetation ones (Fig. 9). First, stacked block properties are calculated. Then, building and vegetation Röckle zones boundaries are identified and the wind factor corresponding to each zone is calculated. Last, some rules are set to keep only one wind factor value when two (or more) Röckle zones overlay.

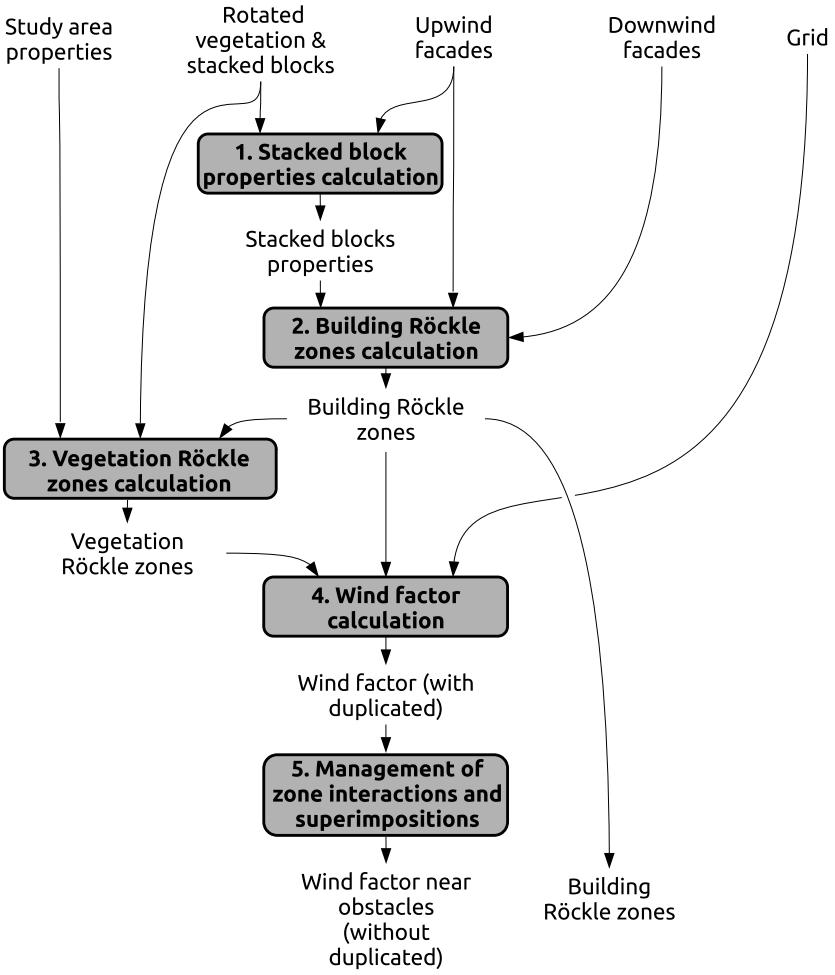

Figure 9. Procedure used to take into account the effect of each individual obstacle on the wind field

2.3.1 Stacked block properties calculation

The stacked block height, effective width (cross-wind width, W_{eff}) and effective length (along wind length, L_{eff}) are the three input parameters used to calculate the building zones. While the definition of the first one have not changed over QUIC-URB versions (difference of height between the top and the base of a stacked block), the definition of the two others have been updated by Nelson et al. (2008) to improve the accuracy of the estimated wind field when the wind was not coming perpendicular to the facade of a rectangular building (Fig. 10).

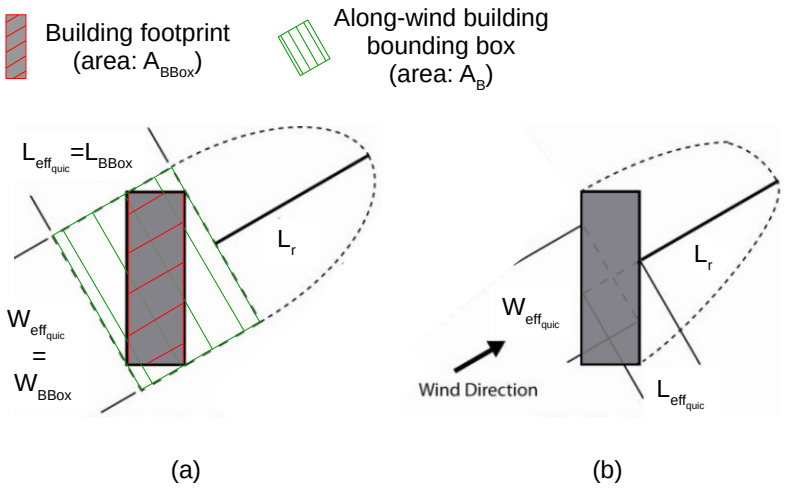

Figure 10. QUIC-URB method to calculate the building effective width and building effective length (a) before and (b) after modifications proposed by Nelson et al. (2008). Source: Adapted from Nelson et al. (2008)

However, their modified algorithm only works for rectangular shape, whereas our stacked blocks may have any shape. Thus, the effective width and length are calculated using ~~respectively~~ Eq. 4 and 5 respectively.

$$W_{eff} = W_{BBox} \cdot \frac{A_B}{A_{BBox}} \tag{4}$$

$$L_{eff} = L_{BBox} \cdot \frac{A_B}{A_{BBox}} \tag{5}$$

where W_{eff} is the effective width of the stacked block in URock~~,~~; L_{eff} is the effective length of the stacked block in URock~~,~~; W_{BBox} is the cross-wind width of the stacked block bounding box (corresponding to $W_{eff_{quic}}$ in Fig. 10a)~~,~~; L_{BBox} is the cross-wind length of the stacked block bounding box (corresponding to $L_{eff_{quic}}$ in Fig. 10a)~~,~~; A_B is the stacked block footprint area (cf Fig. 10a)~~,~~; A_{BBox} is the area of the stacked block bounding box (cf Fig. 10a).

2.3.2 Building Röckle zones calculation

This section contains a partial description of the building Röckle zones calculated in URock. More details can be found in ~~the~~ appendix A.

Displacement zone

The displacement zone is defined as a quarter of ellipse located on each upwind facade (cf Fig. 1a) ~~such~~ as defined by Kaplan and Dinar (1996).

Displacement vortex zone

The displacement vortex zone is defined as a quarter of ellipse located on each upwind facade whenever the angle between the wind direction and an upwind facade normal $\theta_{wind/upwind_F}$ is within [-PERPENDICULAR_THRESHOLD_ANGLE, PERPENDICULAR_THRESHOLD_ANGLE] (cf Fig. 1a). The default value for PERPENDICULAR_THRESHOLD_ANGLE is set to 15°compared to 20°in QUIC-URB (Bagal et al., 2004). The reason for this difference is that the rooftop perpendicular scheme is also activated when the upwind facade is ~~nearby the perpendicular from~~ close to the perpendicular to the wind direction~~but the~~ . The condition for activation of the rooftop perpendicular and displacement vortex differs in QUIC-URB (15°for the rooftop perpendicular while 20°for the displacement vortex) ~~while~~ but we chose to have consistency between these two schemes in URock. ~~However~~Nevertheless, the size of the zone is identical in URock and QUIC-URB (Bagal et al., 2004).

Cavity zone

The cavity zone can be seen as a quarter of ellipse but having a slightly modified equation. If a standard ellipse has a fixed center, the one used in URock has a center ~~which moves upon the along-wind~~ that moves along the wind direction, following the facade coordinates (cf. Fig. 1a). For complex stacked blocks, such as having multiple downwind facades, this definition results in ~~the~~ cavity zones illustrated in Fig. 11. For any downwind facade, the ellipse has the same size at a given coordinate along the cross-wind axis~~(left to right on the Figure)~~. This is most probably not the case in ~~the~~ reality and thus ~~must~~ should be further investigated in future URock versions.

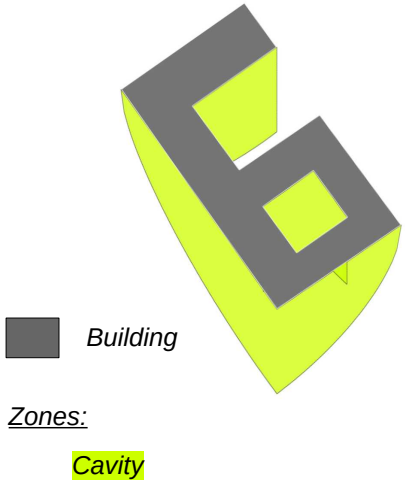

Figure 11. View from the top of the cavity zones created for a complex stacked block

Wake zone

The wake zone ~~comes along with~~ develops after the cavity zone. Thus~~it has exactly the same shape~~, it has a similar shape, but is three times longer ~~along-wind~~ along the wind axis (Kaplan and Dinar, 1996).

Rooftop perpendicular zone

The rooftop perpendicular zone is defined as ~~a half ellipse base cylinder cut along its height and~~ half of an elliptical cylinder ~~—~~ sliced longitudinally along the cylinder axis and major axis of the ellipse. It is located on each rooftop with lengths consistent with the ones defined by Pol et al. (2006). It is only created when the angle between the wind direction and an upwind facade normal $\theta_{wind/upwind_F}$ is within [-PERPENDICULAR_THRESHOLD_ANGLE, PERPENDICULAR_THRESHOLD_ANGLE] (cf Fig. 1a). The default value for PERPENDICULAR_THRESHOLD_ANGLE is set to 15°, the same value as in QUIC-URB (Pol et al., 2006). Note that the rooftop perpendicular zones are only defined above buildings~~and extend along-wind from upwind facades, leading to cylinders having non parallel bottom and top sections~~ . Since they extend from the upper edges of the upwind facades along-wind, they form oblique cylinders whenever the wind is not perpendicular to the upwind facade.

Rooftop corner zone

The rooftop corner zone is defined as a square base oblique pyramid located on rooftop along an upwind facade with the apex starting from the most upwind point (cf Fig. 1a). The size of the zone is calculated using ~~Bagal et al. (2004) equations~~ the equations of Bagal et al. (2004). The scheme is activated only when the angle between the wind direction and an upwind facade normal $\theta_{wind/upwind_F}$ is within +-[~~90+~~CORNER_THRESHOLD_ANGLE_MIN, ~~90+~~CORNER_THRESHOLD_ANGLE_MAX] and the default values for CORNER_THRESHOLD_ANGLE_MIN and CORNER_THRESHOLD_ANGLE_MAX are respectively 30 and 70°.

Street canyon zone

The street canyon zone is created between two stacked blocks when the upstream building cavity zone intersects ~~an~~ the upwind facade of a downstream building.

2.3.3 Vegetation Röckle zones calculation

Similarly as QUIC-URB (Nelson et al., 2009), two different schemes are dedicated to the vegetation in URock: one when the vegetation is located within a building influence (vegetation in built-up area), and the other when ~~is is~~ it is far from building influence (vegetation in open area).

Vegetation in built-up areas

The *vegetation built* zone is defined wherever the wake zone of any building intersects the footprint of a vegetation patch. Only the column of air located within the vegetation canopy belongs to the zone (cf Fig. 1c).

Vegetation in open areas

The *vegetation open* zone is defined wherever the footprint of a vegetation patch is not intersected by any building wake zone. The entire column of air (below, within and above the vegetation) belongs to the zone (cf Fig. 1c).

2.3.4 Wind ~~factors~~ factor calculation

Once the wind zone are defined, wind factors along the three vector components are set. They are defined as the fraction of the wind speed at a given height and position, and are Röckle zone dependent. The equations used to calculate these wind factors are described in appendix B. For a more visual representation of these equations, please refer to the wind field illustrated in Fig. 1.

2.3.5 Management of zone interactions and superimpositions

The ~~philosophy of the URock workflow to deal~~ workflow of URock for dealing with zone interactions and superimpositions is mainly based on QUIC-URB method. For ~~the reader willing to find the main physical motivations for the choice made in the~~ additional details on the adopted method, which also motivated our decisions regarding the URock method, ~~please refer~~ the reader is referred to Brown et al. (2009a, 2013). ~~However, although~~ Although the philosophy and main physical reason for their method are well described, it is difficult to discern a clear algorithm in the QUIC-URB method. This section ~~tries~~ attempts to fill this gap.

Concerning zone interactions, the cavity zone of any stacked block may remove or create zones ~~when some given conditionsare met. In URock , it~~ under certain conditions. URock removes any rooftop zone and any downwind building zone, respectively for the *cavity-rooftop* and *cavity-downwind facade* interactions (Fig. 12a and 12b). Backward cavity and wake zones are also created in the case of the *cavity-upwind facade* interaction (12c). They have the same size as forward cavity and wake zones, except that they start from upwind facades instead of downwind facades and thus, go in the opposite direction. Their wind factor for a same distance from wall and height is also identical ~~as~~ in forward cavity and wake zones, except that they are multiplied by a coefficient of attenuation. The value of this coefficient depends ~~of~~ on the location of the upwind facade within the cavity zone. The value of the cavity zone wind factor at the top of the upwind facade is taken as attenuation coefficient. Backward zone creation removes all downwind zones (cavity, wake, and street canyon), which may be at this position. The definition of the upwind stacked block ~~: it~~ starts from the upper part of the backward zones instead of the ground.

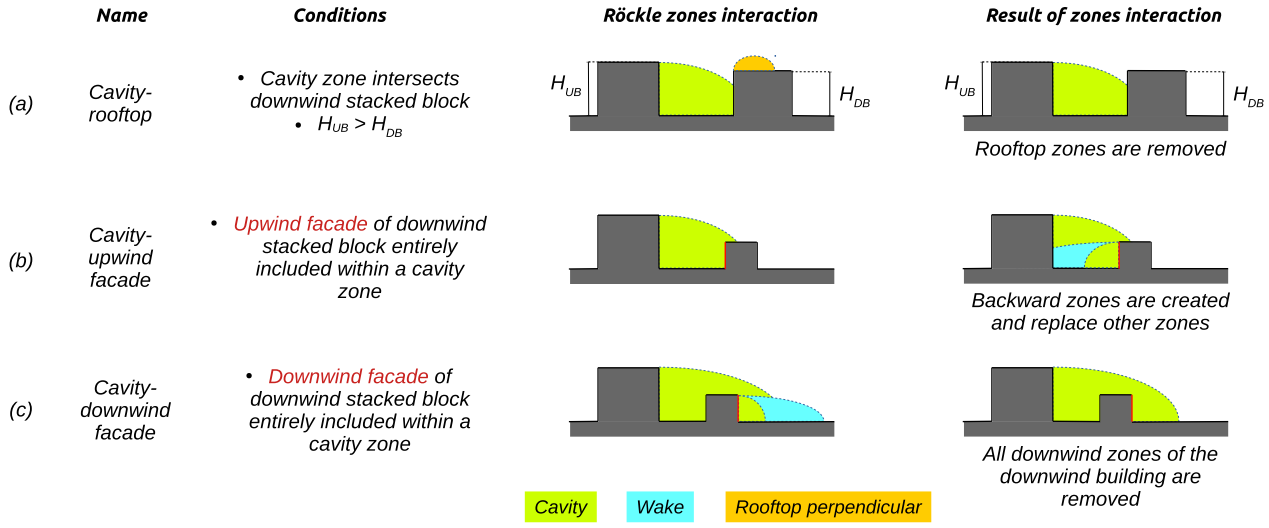

Figure 12. Description and results of the Röckle zone interactions implemented in URock.

Once these interactions are solved, ~~some points of the space may be covered by~~ certain points in the domain may belong to several zones (Röckle zones superimposition). In this case, the following procedure is used to decide what rule or combination of rule apply to each of these points (presented Fig. 13 and further described afterward):

– ~~Only~~ Task 1: only forward building zones superimpositions are solved in order to have a single wind factor per point of the space,

– ~~Similar~~ Task 2: similar work is performed with backward building zones but previously weighted by forward wake zones,

– ~~Forward~~ Task 3: forward and backward wind factors are merged (backward wind factors are used in case of zone intersections),

– ~~The~~ Task 4: the resulting wind factors are multiplied by vegetation weights when they intersect vegetation zones.

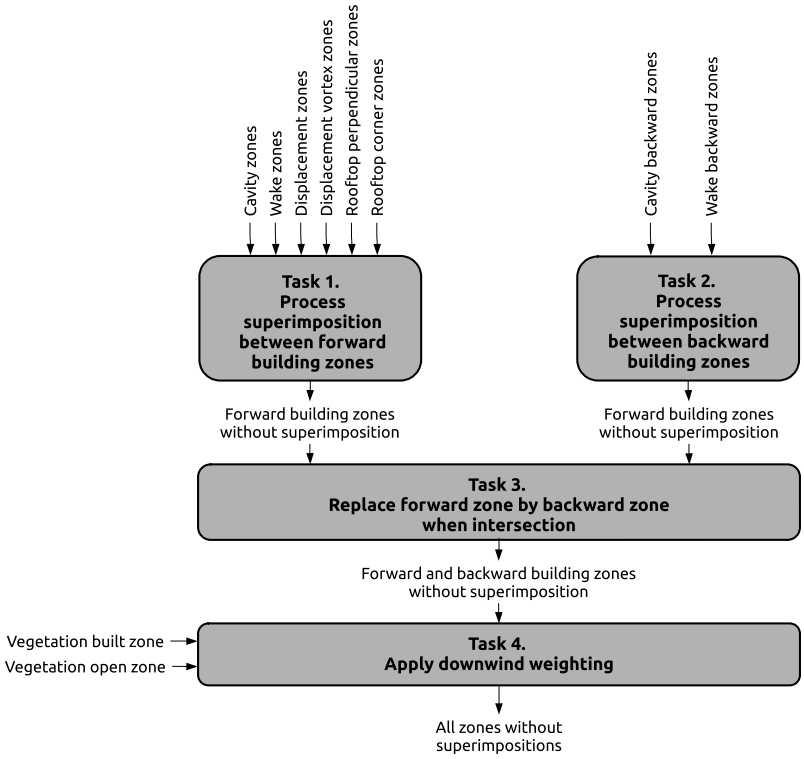

Figure 13. Workflow used to deal with zone superimposition

~~Step 1 consists in three tasks. The first task is to deal with superimposition happening between all building zones . To achieve this, the~~ When several zones are superimposed, most of the choices are based on the *most upstream and tallest stacked block rule*. It means that the zone created by the most upstream stacked block is conserved~~(the~~ . The origin of a zone is defined by the upwind facade for rooftop and displacement zones, and by the downwind one for cavity, wake and street canyon zones~~).~~ ~~If equal~~. If the origin of two zones is the same (i.e. one block piled on an other), then the zone created by the upper stacked block is conserved. If ~~equal~~the zones have been created by a same stacked block, the conserved zone is defined using the following priority order: street canyon, cavity, rooftop perpendicular, rooftop corner, displacement vortex, displacement, wake ~~. The second task~~ zone.

Task 1 consists in three subtasks. The first subtask resolves the superimposition between all building zones based on the previous rule. The second subtask is to deal with superimposition happening only between wake zones. The most upstream and

highest stacked block rules described above is again used. The last ~~task~~ subtask is to multiply the wind factors coming from ~~task~~ subtask 1 by those obtained from ~~task~~ subtask 2 only if those from ~~task~~ subtask 2 come from a more upstream and highest stacked block.

~~Step~~ Task 2 is quite similar to ~~step~~ task 1. The first ~~task is applied using~~ subtask is to resolve backward cavity and backward wake zones, but conserving zones created by the most downstream stacked block instead of the most upstream one. The second ~~task~~ subtask is applied using only backward wake zone using the most downstream stacked block rule. The third ~~task~~ subtask is also a combination of the results from ~~task~~ subtask 1 and ~~task~~ subtask 2 but using the most downstream stacked block rule. ~~A last taskis added using the forward wake zone wind factors (obtained in step 1 task 2) to multiply the results from step 3.~~ The fourth, additional task, is to multiply the wind factors from the previous task 3 with the ones obtained in task 1, subtask 2.

~~Step~~ Task 3 and 4 are simpler~~thus~~ , thus, the description given previously is sufficient to understand what is performed. Fig. 14 illustrates the result of the whole superimposition procedure (considering only ~~5~~ five zone types for the sake of simplicity: vegetation, cavity, wake, backward cavity and backward wake).

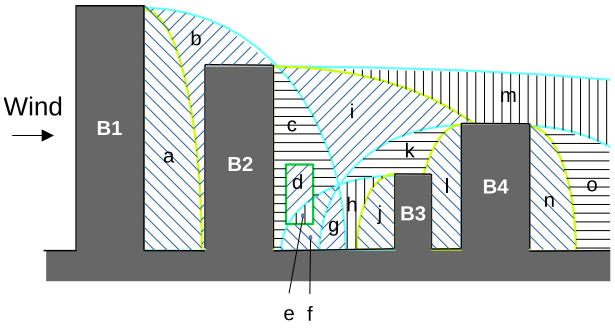

a. *B1 cavity*
b. *B1 wake*
c. *B2 cavity weighted by B1 wake*
d. *B2 cavity weighted by B1 wake and vegetation*
e. *B3 backward wake weighted by B1 wake and vegetation*
f. *B3 backward wake weighted by B1 wake*
g. *B3 backward wake weighted by B4 backward wake and B1 wake*
h. *B3 backward wake weighted by B4 backward wake*
i. *B2 cavity*
j. *B3 backward cavity weighted by B4 backward wake*
k. *B4 backward wake*
l. *B4 backward cavity*
m. *B2 wake*
n. *B4 cavity weighted by B2 wake*
o. *B4 wake weighted by B2 wake*

Figure 14. Example of zones resulting from the superimposition workflow

2.4 Wind speed calculation

The wind speed field calculation is performed in two steps: first, the wind speed is initialized for all points of the domain~~and second~~ , and second, the numeric wind solver is applied to balance the wind flow (Fig. 15).

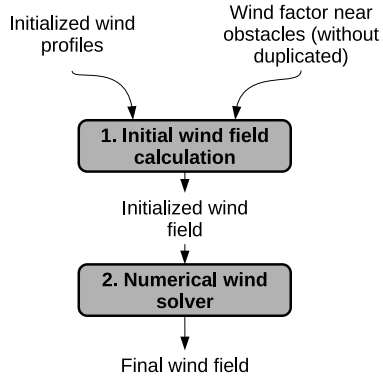

Figure 15. Procedure used to calculates wind speed field from vertical wind profile and wind factors

2.4.1 Initial wind field calculation

Once the wind factors (WF) are calculated and unique for any point of the space, they are used along with the vertical wind profile to initialize the wind speed field using Eq. 6.

$$\begin{cases} U_0(x,y,z) = WF_U(x,y,z) \cdot V_{wp}(x_{ref},y_{ref},z_{ref}) \\ V_0(x,y,z) = WF_V(x,y,z) \cdot V_{wp}(x_{ref},y_{ref},z_{ref}) \\ W_0(x,y,z) = WF_W(x,y,z) \cdot V_{wp}(x_{ref},y_{ref},z_{ref}) \end{cases} \tag{6}$$

where $U_0(x,y,z)$, $V_0(x,y,z)$, $W_0(x,y,z)$ the wind speed respectively along x~~,~~; y and z axis for the point with coordinates x, y, z; $WF_U(x,y,z)$, $WF_V(x,y,z)$, $WF_W(x,y,z)$ the wind factor respectively along x, y and z axis for the point with coordinates x, y, z (default 1 is not covered by any Röckle zone); $V_{wp}(x_{ref},y_{ref},z_{ref})$ the along wind (y-axis) wind speed for the point at the reference position of the zone

Three definitions of $V_{wp}(x_{ref},y_{ref},z_{ref})$ ~~exists~~ exist depending on the zone:

1. ~~the~~ The wind speed is taken at the top of the facade that corresponds to the begining of the zone (note that in the current version of URock, the entire domain has the same vertical wind profile, thus only z_{ref} will affect $V_{wp}(x_{ref},y_{ref},z_{ref})$ value):
   (a) upwind facade for displacement, displacement vortex, backward cavity and backward wake zones,
   (b) downwind facade for cavity and street canyon.
2. ~~the wind speed~~ The wind speed is taken at the location of the point of interest (x, y, z): wake, vegetation built and vegetation open zones (all weighting zones),
3. ~~the wind speed~~ The wind speed is taken at the reference height as used in Eq. B5 and B6 ~~:~~ (rooftop perpendicular and rooftop corner zones).

2.4.2 Numerical wind solver

The last step of the methodology consists in balancing the air flow while minimizing the modifications of the initialized wind field. To achieve this, the Lagrange multiplier (λ) in Eq. 7 is calculated. First, the initial wind field calculated at the center of each voxel is linearly interpolated to the voxel faces. Afterwards, an iterative process is used to calculate the 3D values of λ (for more detail concerning the numerical solver, please see Pardyjak and Brown (2003)).

$$E(u,v,w,\lambda) = \int_V [\alpha_1^2 \cdot (u-u_0)^2 + \alpha_1^2 \cdot (v-v_0)^2 + \alpha_2^2 \cdot (w-w_0)^2 + \lambda \cdot (\frac{\partial u}{\partial x} + \frac{\partial u}{\partial x} + \frac{\partial u}{\partial x})] \cdot dx \cdot dy \cdot dz \quad (7)$$

where $E(u,v,w,\lambda)$ the function to minimize~~,~~; V the whole domain ~~,~~volume; α_1 and α_2 Gaussian precision moduli that can be used to favour modification of the wind field toward horizontal or vertical direction (by default set to 1)~~,~~; u, v, w the balance wind field~~,~~; u_0, v_0, w_0 the initial wind field~~,~~; dx, dy, dz the domain resolution along x, y and z axis

If $\lambda_{i,j,k}^t$ and $\lambda_{i,j,k}^{t+1}$ are λ values for cells located at coordinates i, j, k at iteration steps t and $t+1$ respectively, we stop the iterative process when the condition described Eq. 8 is met.

$$E = \sum_{i=1}^{nx}\sum_{j=1}^{ny}\sum_{k=1}^{nz} |\lambda_{i,j,k}^{t+1} - \lambda_{i,j,k}^{t}| < \epsilon \quad (8)$$

where ϵ the threshold value to stop iterations (default 0.0001)

Last, the wind velocity field is updated using the final λ values (Eq. 9). Note that the wind speed orthogonal to the boundary of a solid cell should be zero ($\frac{\partial \lambda}{\partial n}$) and at the inflow/outflow boundary, the initial wind profile should not be modified ($\lambda = 0$).

$$\begin{cases} u = u_0 + \frac{1}{2 \cdot \alpha_1^2} \cdot \frac{\partial \lambda}{\partial x} \\ v = v_0 + \frac{1}{2 \cdot \alpha_1^2} \cdot \frac{\partial \lambda}{\partial y} \\ w = w_0 + \frac{1}{2 \cdot \alpha_2^2} \cdot \frac{\partial \lambda}{\partial z} \end{cases} \quad (9)$$

3 Model implementation

Currently, URock 2023a is openly available as a QGIS plugin in the Zenodo repository~~(the~~[5]. The tool development is currently performed on GitHub at ~~and will be soon continue at)~~the UMEP repository[6]. It is mainly coded in Python and can be used as a standalone python library. Most of the spatial analysis is performed using the H2GIS spatial database (Bocher et al., 2015). The wind solver is based on the Numba Python library to boost the calculations.

In QGIS, the following minimal informations are needed:

- ~~geographical~~ Geographical informations: one GIS layer for buildings or one for vegetation, with at least a single attribute for roof or crown top height from ground respectively,
- ~~wind~~ Wind conditions: wind speed and direction at a given height or a wind direction and a file containing a wind profile (csv file with height as first column, wind speed as second column),

[5]https://zenodo.org/record/7681245 (last access: 1 August 2023)
[6]https://github.com/UMEP-dev/UMEP-processing (last access: 1 August 2023)

– ~~cell~~ Cell size: the vertical and the horizontal resolution used for the wind solver,

– ~~output~~ Output height: one or several height for which the wind field is needed.

As output, URock 2023a can save the 3D wind field in a NetCDF file or wind information along one or several planes at a height defined by the user in two formats: a raster file, containing the absolute wind speed, or a vector file, containing horizontal wind speed, vertical wind speed, absolute wind speed and wind direction.

~~Soon,~~ URock 2023a ~~will be~~ is integrated within the QGIS plugin called UMEP. Like any UMEP processor, URock comes with its own preprocessor called *urock_prepare* and its own postprocessor called *urock_analyser* (cf. workflow Fig. 16). The first is useful if the user has ~~the~~ building footprint (or vegetation) ~~but~~ without height attribute. If ~~he~~ the user has a Digital Surface Model (for building or vegetation) and a Digital Elevation Model, ~~he can use~~ *urock_prepare* ~~to generate the~~ can be used to generate building and vegetation ~~file~~ files in the right format. The postprocessor is used once URock 2023a has been run (and a NetCDF file saved) to plot a ~~section~~ sectional view of the wind along a line, or a vertical wind profile averaging the wind within a polygon. These two modules are already available ~~on GitHub (at and respectively) but will be soon integrated within the UMEP project~~in UMEP and their development is performed on GitHub[7].

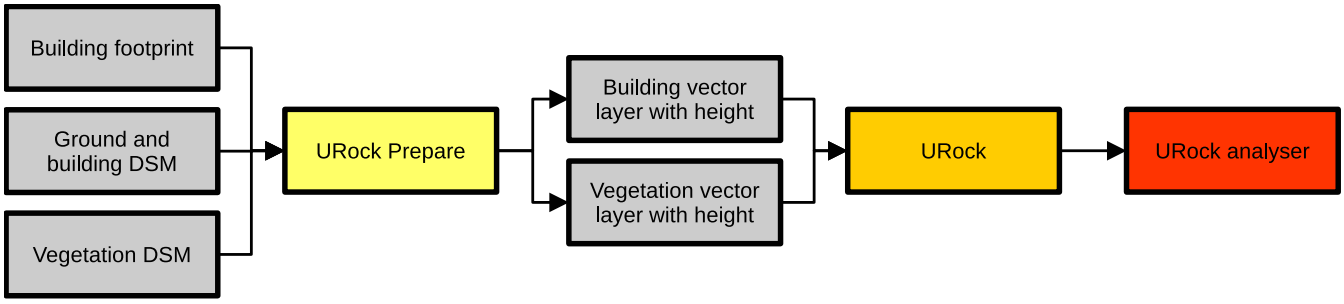

Figure 16. Workflow used to generate and analyse a wind field from raster data using URock and its related preprocessor and postprocessor

4 Model evaluation

In this section, URock (version 0.0.1) simulations are compared to QUIC-URB (version 6.4.1 in Matlab R2020b) simulations and wind tunnel measurements for both simple and more complex cases. Vertical and horizontal resolutions are set identically in URock and QUIC-URB. Preliminary investigations have shown a very limited effect of ~~the resolution on the~~ resolution on accuracy. Thus, the main motivation for the resolution chosen in this paper is to facilitate the visual comparison between the models outputs and the measurements.

Spatial data and vertical wind profiles are set according to wind tunnel experiment parameters. All wind tunnel data are freely available on the AIJ website[8].

[7]https://github.com/UMEP-dev/UMEP-processing (last access: 1 August 2023)
[8]https://www.aij.or.jp/jpn/publish/cfdguide/index_e.htm (last access: 9 December 2022)

Table 2. Domain size used for the URock 2023a model to simulate AIJ cases and associated computation time

AIJ case	Number of cells	Calculation time (s)
AIJ_CaseA	199,778	23
AIJ_CaseB	314,415	23
AIJ_CaseC - from West	667,485	40
AIJ_CaseC - 22.5° clock-wise from West	786,236	33
AIJ_CaseE - 202.5° clock-wise from North	6,379,965	340
AIJ_CaseE - 90° clock-wise from North	5,967,360	318
AIJ_CaseG	280,112	33

The simulations of each AIJ case has been run using the input wind profile measured in the wind tunnel for a given wind direction. The sensors being not necessarily located at the center of a simulation cell, linear interpolation is used in order to compare the wind at the exact sensor location. Figures presented in the next subsections are created using URock and QUIC-URB outputs in QGIS for top view figures and using the module *URock analyzer* for the sectional view figures.

4.1 Computation time

For each of the AIJ cases simulated using the URock model, the number of cells used for the calculation and the computation time are given in Tab. 2. The calculations have been performed using a single processor (frequency of 2.3 GHz) of a personal computer. The installed Random Access Memory of the computer is 16 GB. Note that the time presented also account for file loading (spatial information and wind conditions), initializing connection with the database used for spatial calculation and writing output files.

4.2 General agreement between URock and QUIC-URB

Based on the locations where the wind has been observed in the AIJ wind tunnel experiment, the correlation coefficient calculated between URock and QUIC-URB is shown for horizontal, vertical or absolute wind speed for each of the test cases (Tab. 3).

QUIC-URB and URock show a good agreement for most of the cases. Two cases have particularly low correlation coefficient: case G and the vertical wind speed for case B. For the first case, the low score is ~~only~~ primarily due to the fact that in this case, the spatial variations of the wind speed are very low (thus even a small difference leads to a considerable decrease of the correlation). For the latter case, the low score is mainly explained by ~~only~~ three points having ~~really high value in QUIC while~~ high values in QUIC but low in URock. However, these points are not relevant since they are associated ~~to upward winds~~with upward winds, both in QUIC and URock~~while~~ , but downward winds in the AIJ data (~~further discussed~~ see further discussions in section 4.4).

In the next sections, QUIC-URB results are ~~shown only~~ only shown when they differ ~~sufficiently~~ significantly from URock results. Thus, most ~~of the success~~ successes and limitations that are shown for URock are also applicable for QUIC-URB.

Table 3. Correlation coefficients between URock and QUIC-URB for each AIJ cases

AIJ case	Horizontal	Vertical	Absolute
AIJ_CaseA - 1.25m	0.94	0.71	-
AIJ_CaseA - 12.5m	0.87	0.76	-
AIJ_CaseB - 1.25m	0.99	0.34	-
AIJ_CaseC – 0° from West	-	-	0.88
AIJ_CaseC – 22.5° clock-wise from West	-	-	0.88
AIJ_CaseE – 202.5° clock-wise from North	-	-	0.79
AIJ_CaseE – 90° clock-wise from North	-	-	0.82
AIJ_CaseG	-	-	0.42

4.3 Isolated building - square base

The building used for this case has a square base of size b and its height is twice its width ($h = 2 \cdot b$). More informations about the inflow wind profile and ~~accurate~~ exact sensor location can be found in the *case A* description on the AIJ website and also in MENG and HIBI (1998).

Horizontal wind vectors near the ground show a good agreement between models and observations. The main differences can be observed near the corner of the upwind facade where the cross-wind component is higher in the AIJ data than in URock. Absolute horizontal wind speed generally agree except in an along-wind ellipse located right beside the building edge (red ellipse Fig. 17a). Due to the absence of Röckle zone in this area, URock overestimates the wind speed (Fig. 17c).

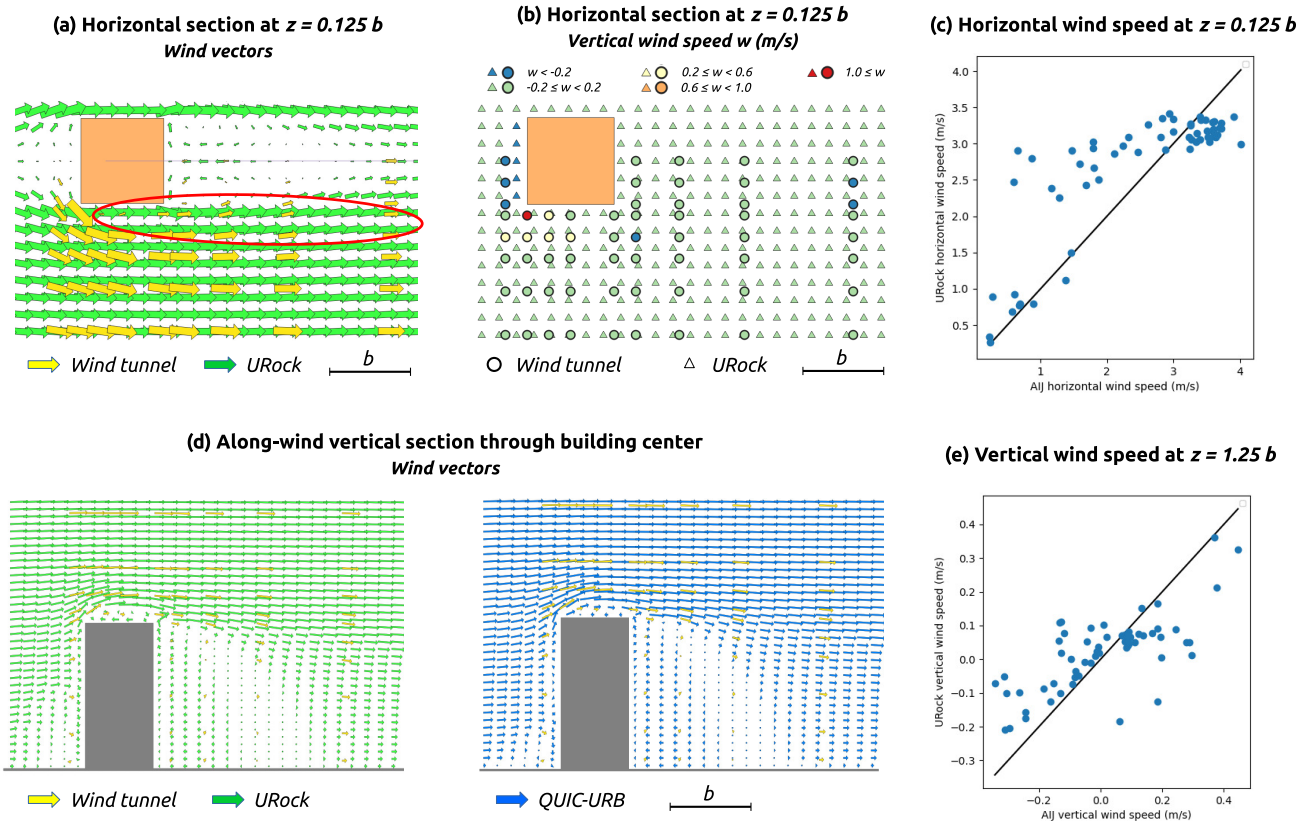

Figure 17. AIJ wind tunnel measurement as well as URock and QUIC-URB outputs for a square base isolated building

Near the ground ($z = 0.125 \cdot b$), URock vertical wind speed values are ~~really low (included~~ low (remaining between -0.15 and 0.05 m/s), while observations show ~~quite high wind speed locally (below 0.5 and above~~ a higher wind speed range (from -0.5 to 1.5 m/s). The main spatial difference is located near the upwind edges of the building: the displacement vortex that goes cross-wind along the upwind facade is known to continue its way up and along-wind when it reaches the building corner. This leads to a non-negligible vertical component in this area as we can see in Fig. 17b.

At higher level ($z = 1.25 \cdot b$), the absolute vertical wind values observed are lower (below 0.5 m/s) and URock captures well the spatial variability of the AIJ values (Fig. 17e).

Wind tunnel measurements have also been performed within an along-wind sectional plane located on the building center. The wind vectors in URock and QUIC-URB are quite consistent with those observed in the AIJ data. The main difference is located at the top of the roof where a clear vortex structure is created in URock while it does not exist (or is limited in size) in the wind tunnel observation and in QUIC-URB (Fig. 17d).

4.4 Isolated building - rectangular base

The building used for this case has a rectangular base of width b (along-wind) and length equal to $4 \cdot b$ (cross-wind), while its height is also $4 \cdot b$. More informations about the inflow wind profile and ~~accurate~~ exact sensor location can be found in the *case B* description on the AIJ website.

URock model has the same qualities and shortcomings for the rectangular ~~than~~ as for the square base case, except that the following shorcomings are exacerbated. First, the cross-wind component of the AIJ vectors near the building corner is higher than the along-wind one~~and this~~. This affects the wind direction of most ~~of the~~ wind vectors downstream (Fig. 18a). Second, the ~~ellipse~~ ellipse-shaped are impacted by wind speed overestimation is slightly wider than previously.

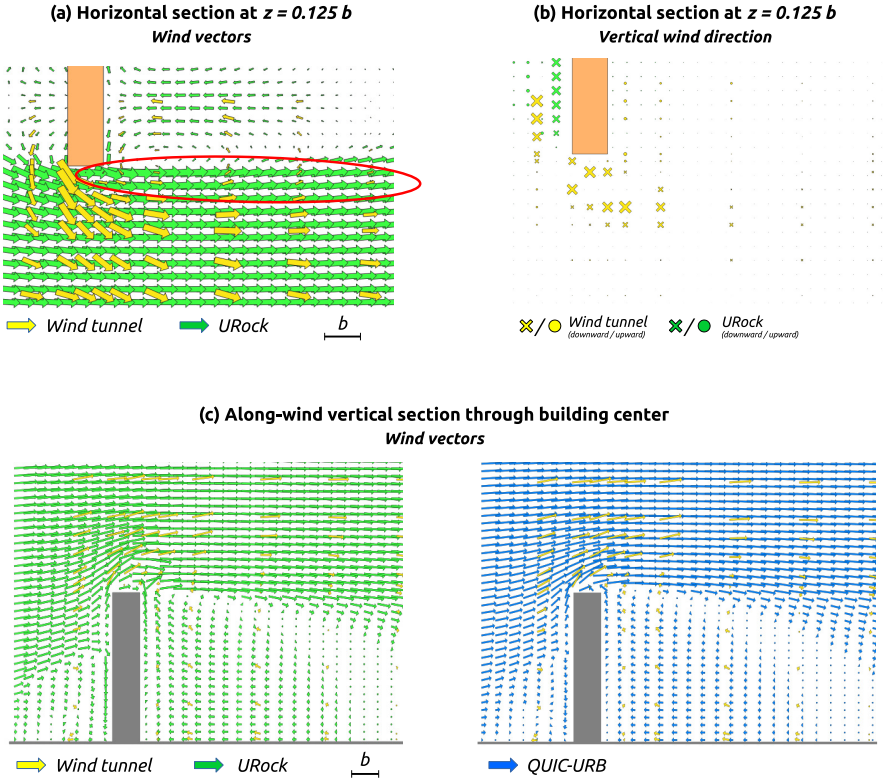

Figure 18. AIJ wind tunnel measurement as well as URock and QUIC-URB outputs for a rectangular base isolated building

One of the reasons for having low values for the cross-wind component near the building corner might come from ~~an~~ the underestimation of downward wind in the displacement zone. In QUIC-URB and URock, a vortex is initialized in front of the upwind facade. This ~~result~~ results in an downward wind close to the wall and an upward wind more upwind. According to Fig. 18b, it seems ~~either~~ that this zone is either not relevant, ~~either~~ or it has to be modified in order to have a downward wind where it currently has an upward wind.

The sectional plot shows a clear wind speed decrease ~~of~~ in the AIJ measurement above the building cavity zone (in the rooftop zone and its prolongation~~- red ellipse -~~; red ellipse in Fig. 18c). This zone do not correspond to any Röckle zone~~and thus~~. Thus, it is overestimated by the URock model ~~(and also the~~ and also by QUIC-URB~~one)~~. In the square and rectangular building cases, the displacement zones differ between URock and QUIC-URB: they are bigger in URock. While it does not impact ~~much~~ the wind field much in the square building case (Fig. 17d), the differences are more pronounced in the rectangular case: the wind speed and direction near the ground is more consistent between URock and the AIJ data than ~~in~~ between QUIC-URB and the AIJ data (Fig. 18c).

4.5 Regularly distributed cubes

The nine cubic buildings used ~~for~~ in this case are regularly distributed in ~~three rows of three buildings~~a 3 x 3 layout. The distance separating each building is equal to the building width. More informations about the inflow wind profile and ~~accurate~~ exact sensor location can be found in the *case C* description on the AIJ website. Note that for this experiment, only the absolute wind speed is measured.

When the wind comes from the ~~West~~west, the scatterplot of URock versus AIJ wind speed looks quite similar ~~as~~ to the one obtained for a single isolated building (Fig. 17c): half of the points ~~follows well a (green) line~~ follow the green regression line that is parallel to the ~~$y = x$~~ identity line and the other half is above this line (Fig. 19b). Most of the points located above the line belong to the area indicated by red ellipses drawn Fig. 19a. A reduction of the wind speed in these zones may then have a double positive impact: first the points have a good chance to get closer to the green ~~dash~~ line and second a reduction of the wind speed at the entrance of the streets may decrease the wind speed of all locations, thus decreasing the positive bias of the current URock version.

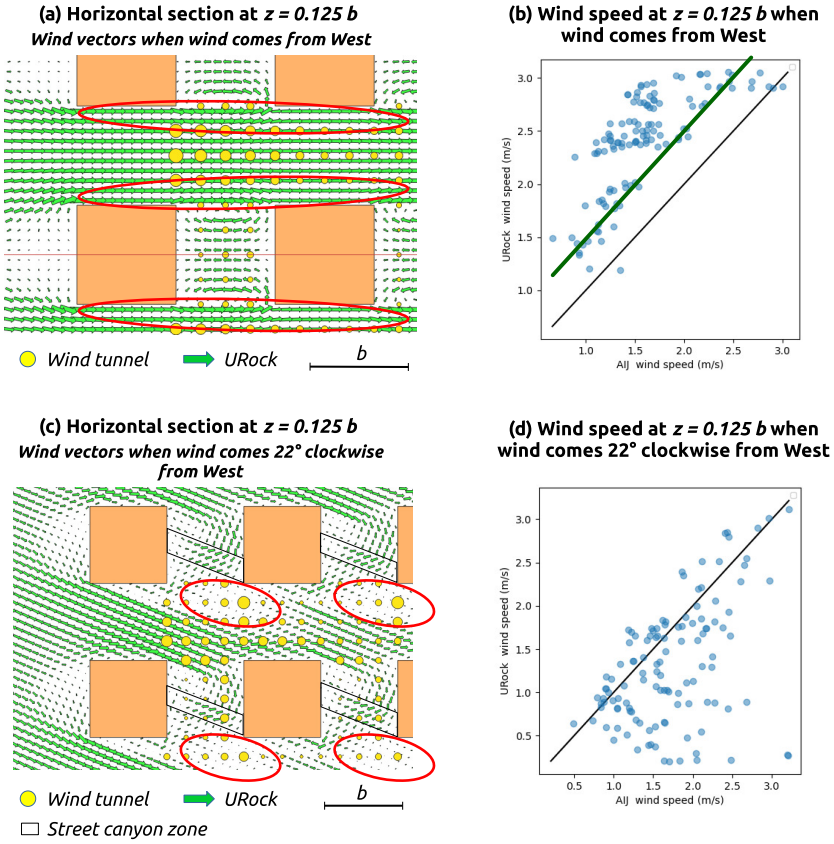

Figure 19. AIJ wind tunnel measurement and as URock outputs for regularly distributed cubes

When the wind comes 22.5° clockwise from the ~~West~~west, a large fraction of the ~~location~~ domain has a good agreement between URock output and observations (Fig. 19d). However, a non-negligible fraction of points are clearly underestimated by URock. The largest ~~fail~~ discrepancies is located downwind ~~most of the~~ to most buildings, at the boundary between their cavity and wake ~~zone~~ zones (Fig. 19c). These underestimated zones are also downstream ~~a small ray~~ to a small set of street canyon zone. The ~~conjonction~~ superimposition of these zones ~~induces~~ results in a really small wind speed at the initialization stage (cavity/wake zone boundary)~~and no reason to get a much~~ , without any rational to reach higher wind speed after the mass-balance stage since the wind ~~in~~ emanating from the street canyon ~~zone is heading toward an other direction than the~~ zones largely avoid the area indicated by red ellipses.

4.6 Isolated tree

The tree used for this case has a 2 m width square base, its crown ~~being located~~ starts from 1.2 m above ground level and extends up to 7 m. Its trunk is considered to have a negligible effect thus it is not represented in URock. More informations about the inflow wind profile and ~~accurate~~ exact sensor location can be found in the *case G* description on the AIJ website.

In URock, a single isolated tree induces only a really small decrease ~~of its~~ in the downward wind speed. On the contrary, the AIJ wind tunnel data shows a considerable decrease: at 3 m ~~high~~height, the wind speed is reduced ~~by~~ to about half of its initial value between 10 and 40 m downstream the tree (Fig. 20). The same level of magnitude is obtained by Li et al. (2023) when simulating ~~(~~via a CFD model ~~)~~ the wind around a ~~tree canopy of~~ 3.6 m wide, 3.6 m ~~length~~ long and 5 m ~~high~~tall tree canopy. Recently, Margairaz et al. (2022) updated the GES-Winds vegetation model for isolated trees~~: they~~ . They have replaced the initial QUIC-URB vegetation model by a new one ~~having~~ that has a wake zone downwind the tree. This model seems to show much better performance than the initial one. Further wind tunnel or observations ~~should be used to comfort this result~~are needed to confirm this result, but it seems that the vegetation zone model used in URock and QUIC-URB ~~needs~~ is not appropriate for isolated trees and need to be updated.

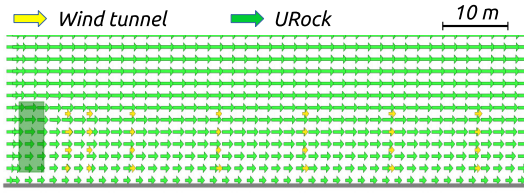

Figure 20. Wind vectors in an along-wind sectional plane located on the tree center: comparison between URock and AIJ wind tunnel measurement

4.7 Real urban setting

~~A~~ The real urban setting ~~is used : it~~ used is a quite large city block with compact low-rise buildings. The wind tunnel observations are available for two cases: a potential future urban setting with three new high-rise buildings located on three existing large courtyards, and the current urban setting with only the existing low-rise buildings. The first case has been chosen for URock evaluation. More informations about the location and size of the buildings, the inflow wind profile and the ~~accurate~~ exact sensor location can be found in the *case E* description on the AIJ website or in Tominaga et al. (2005). Note that for this experiment, only the absolute wind speed is available.

When the wind comes from the East, the correlation between URock and AIJ windspeed is quite good~~, the scatterplot is quite close from the $y = x$ linealthough slightly below~~ . The points on the scatterplot are rather close to the identity line, although located slightly below it (Fig. 21b). ~~However, about~~ About 10% of the ~~locations~~ values are outliers: ~~a major part~~ the majority of them are overestimations (yellow triangles) and three points are underestimations (yellow diamond). Most of these points are located in the largest ~~East North East street~~ street running east-northeast direction (Fig. 21a). Overestimation occurs on the northern part of the street, while the underestimations are located at the intersection with the courtyard where ~~is located~~ the highest building (60 m high) is located.

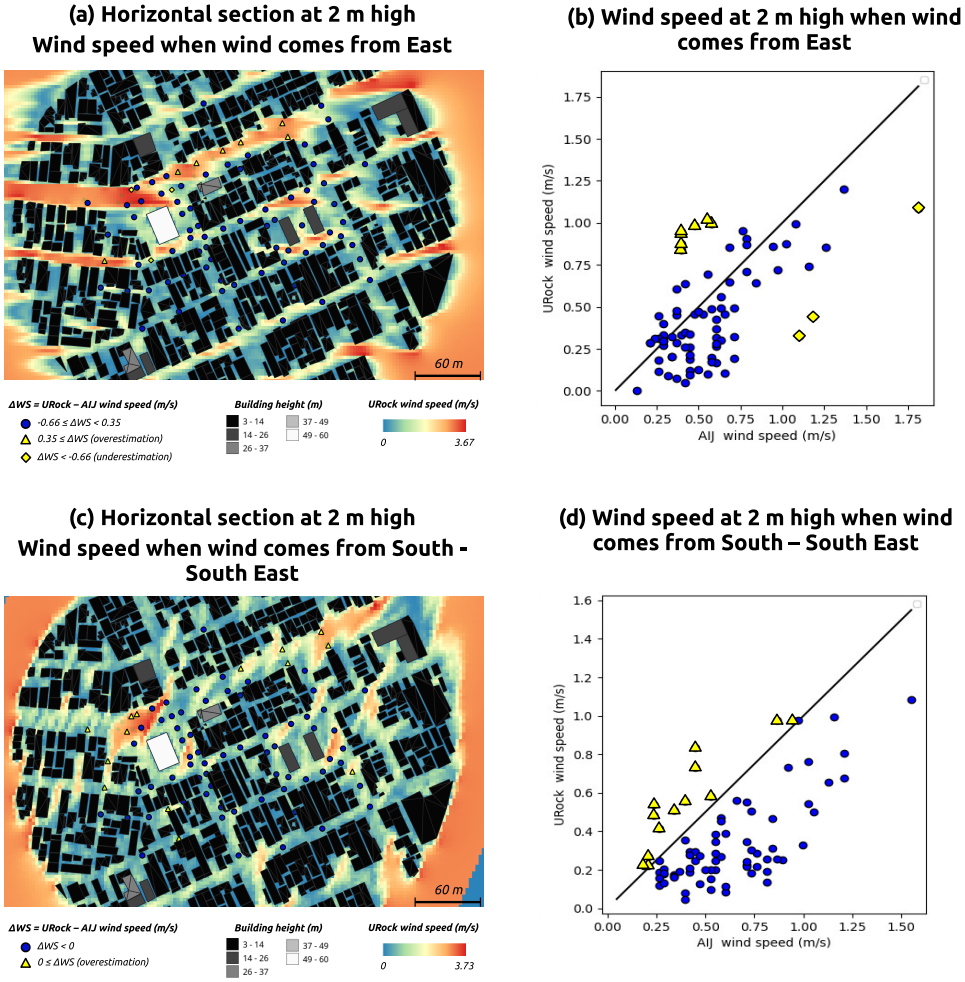

Figure 21. Comparison between URock outputs and AIJ wind tunnel measurement for a real urban setting at 2 m high

When the wind comes from the ~~South-South-West~~ south south-west direction, the correlation between URock and AIJ windspeed is also ~~quite~~ good. There is a more pronounced underestimation of the wind speed, which is quite similar for all AIJ wind speeds (Fig. 21d). Almost 20% of the ~~locations~~ values are outliers (yellow triangles). All of them are overestimations~~and are~~ , and most of them are located far from high-rise buildings (Fig. 21c). Most of them are also outside any building influence (quite far downwind from any building), even though it is not the case for all locations. The central part of the zone, equipped with wind sensors~~is not concerned~~ , is not influenced by these outliers. Thus, the spatial variations in the zone of interest are quite well reproduced by URock, even though there is a general underestimation.

5 Conclusion and discussions

Most models dedicated to the calculation of wind speed in urban settings are intended ~~to specialists,~~ for specialists, are computationally intensive or ~~implemented into~~ are implemented in proprietary softwares. The model presented in this manuscript (URock 2023a) ~~will soon be~~ is available in the free and open source QGIS software ~~within~~ in the UMEP plug-in. Its method is based on the so-called Röckle approach: first, the wind field near obstacles is initialized according to empirical rules drawn from wind tunnel observations ~~;~~ and second, the air flow is balanced minimizing the modification of the initial wind field. This method is reputated as quick but ~~at~~ to our knowledge, only proprietary implementations exist. URock 2023a model is based on the Röckle zones implemented in the state of the art QUIC-URB software. The model ~~method and implementation are described~~ methods and implementations are described in Sect. 2 and 3~~respectively. Its~~ , respectively. The evaluation is performed using both wind tunnel measurement (from the AIJ) and QUIC-URB outputs. This is a good opportunity to show that the results obtained with URock are *(i)* very close ~~from~~ to the ones obtained ~~with~~ using QUIC-URB, *(ii)* close ~~from~~ to the ones obtained ~~in~~ by the wind tunnels experiments for most cases, and *(iii)* open to improvements in some cases (~~further~~ as described below).

In the isolated building cases (section 4.3, 4.4), the wind speed above the building and downstream do not ~~perfectly fit~~ fit perfectly the wind tunnel data. In the square base case, it seems that the rooftop perpendicular zone is too ~~much high~~ tall while in the rectangular base case~~it seems~~ , it seems that the rooftop perpendicular zone should extend not only above the roof but also above the cavity zone (Fig. 18c). Currently, a rooftop zone ~~stops~~ ends when the roof ends, even though the initial zone length is longer. A potential improvement could be to keep the rooftop zone, even though it is wider (along-wind) than the building width.

In the third case, when the wind comes from 22.5° clockwise from the left, ~~some~~ small street canyons are created. The wind direction in these zones might not be ~~appropriate and~~ accurate, which might be partially responsible for the nearby wind speed underestimations. In this configuration, where the street canyon concept is not quite applicable ~~(~~due to a very limited street canyon length~~)~~, the wind flow should be modified in order not to have a ~~brutal~~ drastic change of wind direction. Wind tunnel experiments, where the effect of length of the street canyon is investigated, could be a good dataset for model improvements.

In the first three cases (section 4.3, 4.4 and 4.5), the agreement between the URock field and the wind tunnel data is quite good. Most of the differences observed might be attributed to the high wind speed values located in ~~an~~ the along-wind ~~ellipse~~ ellipse-shaped area starting from the upwind corner of the building. This zone is not defined as a Röckle zone~~while decreasing its wind speed at~~ , although decreasing the wind speed here during the initialization stage could solve most of the problems ~~thanks to~~ as a result of the mass-balance process:

- reduction of the final wind speed in this zone (Fig. 17),
- increase of the cross-wind component near the upwind corner (Fig. 17a),
- increase of the vertical component near the upwind corner (Fig. 17),
- decrease the global flow rate entering the streets and thus reducing the wind speed in most locations (Fig. 19a).

As a first attempt, a solution could also be only to delete the displacement vortex zone or set a downward wind in the displacement zone. Indeed, the analysis of the rectangular base case (B) showed that both URock and QUIC-URB have an upward wind where AIJ data show downward. This ~~modification~~ change may lead to modification in the upstream wind, even though we do not expect it to solve all the ~~problem~~problems.

The isolated tree case does not show a good agreement with the wind tunnel data~~(which are conforted by other literature results)~~. It should be further verified using ~~other~~ additional wind tunnel or observation data and ~~lead to modification of the vegetation Röckle zones if needed~~the Ro¨ckle vegetation zones modified, if necessary.

There is a general wind speed underestimation when ~~we compare URock~~ URock is compared with a compact urban setting. ~~This result seems to~~ Similar results have been identified in ~~previous work (Girard et al., 2018)~~a previous work by Girard et al. (2018). It seems that this behavior is exacerbated when the number of upstream buildings increases (direction SSW compared to E). While it seems that the spatial variations are quite well reproduced, investigations could be carried out to solve this limitation: the vertical wind profile could be updated to take into account the morphometric characteristics of the urban setting.

Outside these model improvements, the model is currently limited to flat areas. A ~~next~~ future version will account for complex ~~terrain~~terrains, taking into account the ~~last literature updates on the field (Robinson et al., 2023).~~latest literature in the field (e.g. that of Robinson et al. (2023)).

Code and data availability. The comparison between model outputs (URock, QUIC-URB) and observation (AIJ wind-tunnel experiments) can be partially reproduced. The QUIC-URB model being a proprietary software, only its output wind fields can be shared. The corresponding files are permanently available on Zenodo at https://zenodo.org/record/7681245, along with the spatial data for each AIJ case (A, B, C, E and G), the URock 2023a software and all scripts needed for running the AIJ cases and comparing QUIC-URB, URock and AIJ wind fields. More information about the step-by-step procedure to reproduce the results can be found in the Readme file of the Zenodo repository.

Appendix A: Calculates building Röckle zones

This section contains more details about some of the building Röckle zones as calculated in URock.

Displacement zone

The displacement zone is defined as a quarter of ellipse located on each upwind facade (cf Fig. 1a). The radius of the ellipse along the facade direction is half the facade length, the radius along the axis perpendicular to the facade (L_f) is defined by Eq. A1 and the vertical radius is 60% of the upwind facade height (H_F) (Kaplan and Dinar, 1996).

$$L_f = 1.5 \cdot \frac{W_{eff}}{1 + 0.8 \cdot \frac{W_{eff}}{H_F}} \tag{A1}$$

Displacement vortex zone

The displacement vortex zone is defined as a quarter of ellipse located on each upwind facade whenever the angle between the wind direction and an upwind facade $\theta_{wind/upwind_F}$ is within [90-PERPENDICULAR_THRESHOLD_ANGLE, 90+PERPENDICULAR_THRESHOLD_ANGLE] (cf Fig. 1a). The size of the zone is identical in URock and QUIC-URB: the radius of the ellipse along the facade direction is half the facade length, the radius along the axis perpendicular to the facade (L_fv) is defined by Eq. A2 and the vertical radius is 50% of the upwind facade height (H_F) (Bagal et al., 2004).

$$L_{fv} = 0.6 \cdot \frac{W_{eff}}{1 + 0.8 \cdot \frac{W_{eff}}{H_F}} \tag{A2}$$

Cavity zone

The cavity zone can be seen as a quarter of ellipse but having a slightly modified equation. If a standard ellipse has a fixed center, the one used in URock has a center which moves upon the along-wind direction, following the facade coordinates (cf. Fig. 1a). The Eq. A3 gives the modified ellipse coordinates for a wind paralell to the y-axis (in URock, all geometries are rotated in order to have wind coming along the y-axis - cf Sect. 2.1.2):

$$\frac{x^2}{W_{BBox}^2} + \frac{(y - y_{0_F}(x))^2}{L_r^2} + \frac{z^2}{H_F^2} = 1 \tag{A3}$$

where

x the coordinate of the ellipse along the x-axis

W_{BBox} the radius of the ellipse along x (corresponding to the cross-wind width of the stacked block)

y the coordinate of the ellipse along the y-axis

$y_{0_F}(x)$ the y-coordinate of the facade (may vary along the x-axis)

L_r the radius of the ellipse along y, defined by Eq. A4

z the coordinate of the ellipse along the z-axis

H_F the radius of the ellipse along z (corresponding to the facade height)

$$L_r = 1.8 \cdot \frac{W_{eff}}{(\frac{L_{eff}}{H})^{0.3} \cdot (1 + 0.24 \cdot \frac{L_{eff}}{H}))} \tag{A4}$$

Rooftop perpendicular zone

The rooftop perpendicular zone is defined as a half ellipse base cylinder cut along its height and located on each rooftop. It is only created when the angle between the wind direction and an upwind facade $\theta_{wind/upwind_F}$ is within [90-PERPENDICULAR_THRESHOLD_ANGLE, 90+PERPENDICULAR_THRESHOLD_ANGLE] (cf Fig. 1a). The cylinder height is the length of the upwind facade, the vertical diameter H_{cm} and the diameter perpendicular to the upwind facade d_{cp} are defined respectively by Eq. A5 and A6 (Pol et al., 2006).

$$H_{cm} = 0.22 \cdot (0.67 * MIN(H_F, W_{eff}) + 0.33 \cdot MAX(H_F, W_{eff})) \tag{A5}$$

$$\begin{cases} d_{cp} = L_{cp} \cdot sin(\theta_{wind/upwind_F}) \\ L_{cp} = 0.9 \cdot (0.67 * MIN(H_F, W_{eff}) + 0.33 \cdot MAX(H_F, W_{eff})) \end{cases} \quad \text{(A6)}$$

Rooftop corner zone

The rooftop corner zone is defined as a square base oblique pyramid located on rooftop along an upwind facade with the apex starting from the most upwind point (cf Fig. 1a). The pyramid height is equal to the length of the upwind facade (L_{fc}), while the width of the pyramid base (L_{cc} is defined by Eq. A7 (Bagal et al., 2004).

$$L_{cc} = 2 \cdot L_{fc} \cdot tan(2.94 \cdot exp(0.0297 \cdot (|\theta_{wind/upwind_F}| - \frac{\pi}{2})) \quad \text{(A7)}$$

where $\theta_{wind/upwind_F}$ is the angle between the wind direction and an upwind facade (in radian)

Appendix B: ~~Calculates~~ Calculation of wind factors

Wind factors along the three components are defined as fraction of the wind speed at a given height and position and are Röckle zone dependent. In this section, the ~~Eq.~~ equations used to calculate these wind factors are described. For a more visual representation of these equations, please refer to the wind field illustrated in Fig. 1.

Displacement zone

In the displacement zone, the wind factors are defined according to Eq. B1 where $z < H_d$ Bagal et al. (2004).

$$\begin{cases} \frac{V_0(z)}{V_p(H_F)} = \frac{U_0(z)}{V_p(H_F)} = C_{dz} \cdot (\frac{z}{H_F})^p \\ H_d = 0.6 \cdot H_F \cdot \sqrt{(1 - \frac{D_y^2}{D_{od}^2})} \end{cases} \quad \text{(B1)}$$

where (cf Fig. B1):

D_y distance to wall along y axis

H_d ellipsoid height at the distance D_y

$C_{dz} = 0.4$

$p = 0.16$

z level of the cell

D_{od} length of ellipsoid along y axis at z = 0 m

θ angle between wind direction and perpendicular to the building wall

H_F building facade height

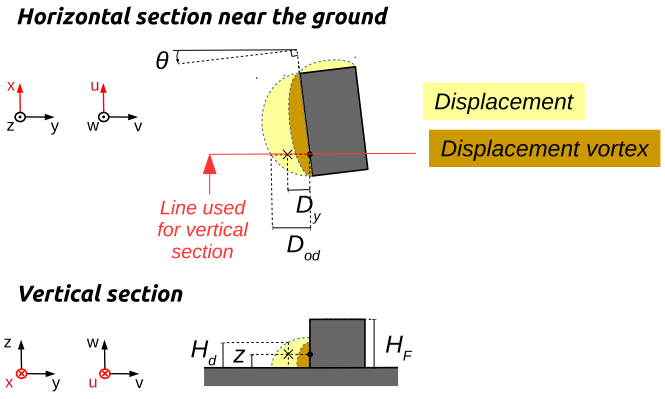

Figure B1. Variables needed for wind factor calculation in displacement zones

Displacement vortex zone

In the vortex zone, the wind factors are defined according to Eq. B2 where $z < H_{dv}$ (Bagal et al., 2004).

$$\begin{cases} \frac{V_0(z)}{V_p(H_F)} = -[0.6 \cdot cos(\frac{\pi \cdot z}{0.5 \cdot H_F}) + 0.05] \cdot 0.6 \cdot sin(\frac{\pi \cdot D_y}{D_{odv}}) \\ \frac{W_0(z)}{V_p(H_F)} = -[0.1 \cdot cos(\frac{\pi \cdot D_y}{D_{odv}}) + 0.05] \\ H_{dv} = 0.5 \cdot H_F \cdot \sqrt{(1 - \frac{D_y^2}{D_{odv}^2})} \end{cases} \quad \text{(B2)}$$

where (cf Fig. B2):

Dy distance to wall along y axis

H_{dv} ellipsoid height at the distance D_y

$C_{dz} = 0.4$

$p = 0.16$

z level of the cell

D_{od} length of ellipsoid along y axis at z = 0 m

θ angle between wind direction and perpendicular to the building wall

H_F building facade height

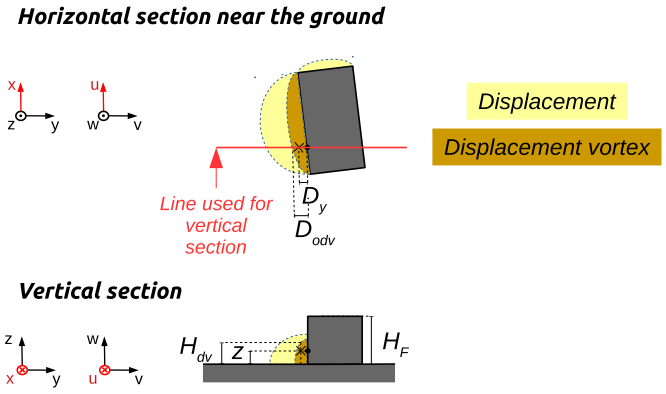

Figure B2. Variables needed for wind factor calculation in displacement vortex zones

Cavity zone

In the cavity zone, the wind factors are defined according to Eq. B3 where $z < H_c$ (Kaplan and Dinar, 1996).

$$\begin{cases} \frac{V_0(D_y,z)}{V_p(H)} = -(1 - \frac{D_y}{D_{oc}\sqrt{1-\frac{z^2}{H^2}}})^2 \\ H_c = H \cdot \sqrt{1 - \frac{D_y^2}{D_{oc}^2}} \end{cases} \tag{B3}$$

where (cf Fig. B3):

D_y distance to wall along y axis

H_c ellipsoid height at the distance D_y

z level of the cell

D_{oc} length of ellipsoid along y axis at z = 0 m

H stacked block height

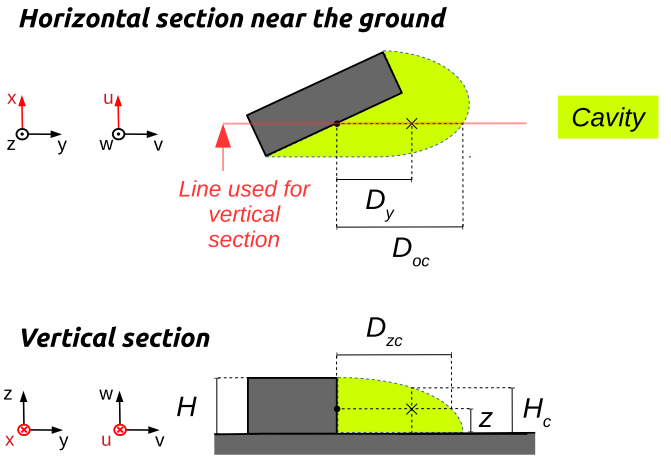

Figure B3. Variables needed for wind factor calculation in cavity zones

Wake zone

In the vortex zone, the wind factors are defined according to Eq. B4 where $z < H_w$ (Kaplan and Dinar, 1996).

$$\begin{cases} \frac{V_0(D_y,z)}{V_p(z)} = -[1-(\frac{D_{oc}}{D_y})^{1.5}\sqrt{1-\frac{z^2}{H^2}}^{1.5}] \\ H_w = H \cdot \sqrt{1-\frac{D_y^2}{D_{ow}^2}} \end{cases} \tag{B4}$$

where (cf Fig. B4):

620 D_y distance to wall along y axis

H_w ellipsoid height at the distance D_y

z level of the cell

D_{ow} length of ellipsoid along y axis at $z = 0m$

H stacked block height

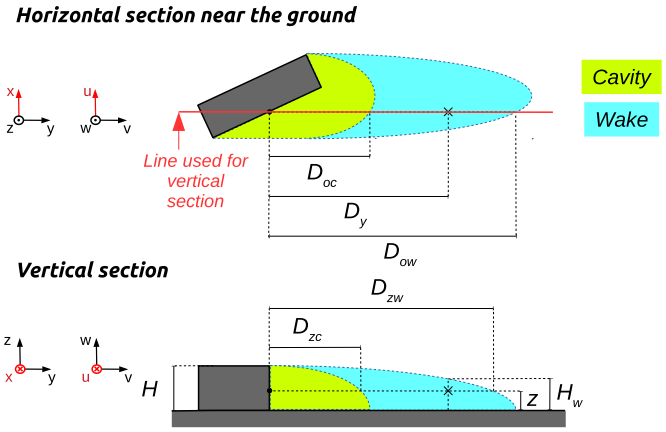

Figure B4. Variables needed for wind factor calculation in wake zones

Rooftop perpendicular zone

In the vortex zone, the wind factors are defined according to Eq. B5 where $H < z < H + H_r$ (Pol et al., 2006).

$$\begin{cases} \frac{V_0(D_y,z)}{V_p(z_{ref})} = -(\frac{H+H_r-z}{z_{ref}})^p \cdot |\frac{H+H_r-z}{H_r}| \\ H_r = H_{cm} \cdot \sqrt{1-(\frac{D_y-\frac{L_{cp}}{2}}{L_{cp}})^2} \end{cases} \tag{B5}$$

where (cf Fig. B5):

$p = 0.16$

$V(z_{ref})$ wind speed at measurement height z_{ref}

D_y distance to wall along y axis

H_r ellipsoid height at the distance D_y

H_{cm} maximum ellipsoid height

L_{cp} rooftop perpendicular length

z level of the cell

H facade height

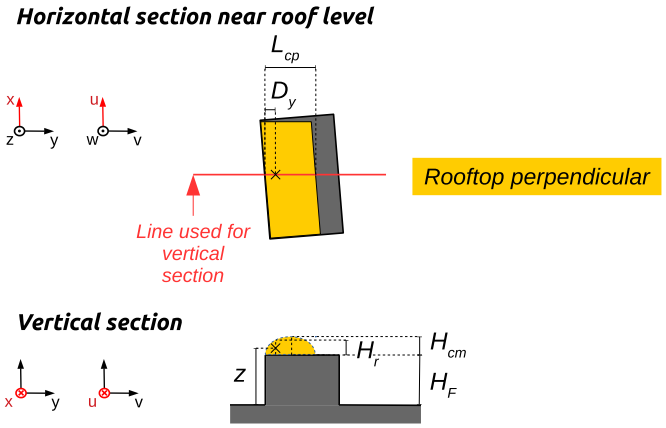

Figure B5. Variables needed for wind factor calculation in rooftop perpendicular zones

Rooftop corner zone

In the vortex zone, the wind factors are defined according to Eq. B6 where $H < z < H + H_{ccp}$ (Pol et al., 2006).

$$\begin{cases} \frac{U_0(D_y,z)}{V_p(z_{ref})} = -C1 \cdot (\frac{H+H_{ccp}-z}{z_{ref}})^p \cdot |\frac{H+H_{ccp}-z}{H_{ccp}}| \cdot sin(2 \cdot \Theta) \\ \frac{V_0(D_y,z)}{V_p(z_{ref})} = -C1 \cdot (\frac{H+H_{ccp}-z}{z_{ref}})^p \cdot |\frac{H+H_{ccp}-z}{H_{ccp}}| \cdot sin^2\Theta \\ H_{ccp} = L_{ccp} = \frac{L_{cc} \cdot \sqrt{x_{L_p}^2 + y_{L_p}^2}}{L_{fc} \cdot cos(\Theta - \widehat{SOP})} \\ C1 = \frac{1+0.05*W_{eff}}{H_F} \end{cases} \quad \text{(B6)}$$

where (cf Fig. B6):

$C1$ wind speed factor

H_F facade height

W_{eff} stacked block effective length

$V(z_{ref})$ wind speed at measurement height zref

H_r ellipsoid height at the distance D_y

H_{ccp} the H_{ccx} value for point p

L_{ccp} the L_{ccx} value for point p

L_{fc} the facade length

L_{cc} the L_{ccx} value at the end of the facade length

$x_{L_{cp}}$ and yLcp absolute coordinates of vector Lccp

z level of the cell

θ angle between wind direction and perpendicular to the building wall

$\widehat{SOP}$ the angle between points S, O and P

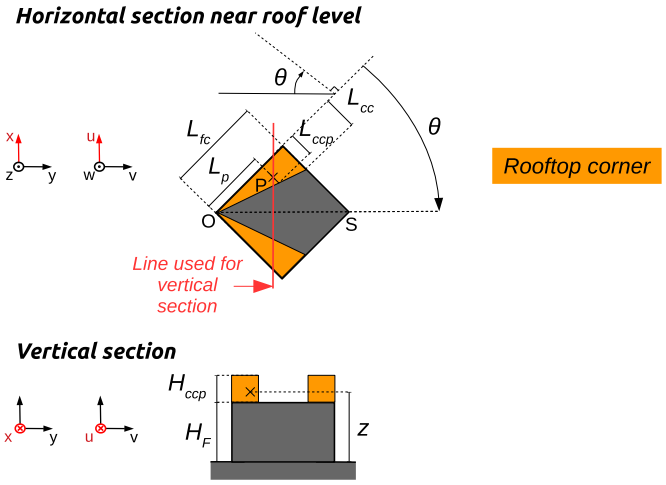

Figure B6. Variables needed for wind factor calculation in rooftop corner zones

Street canyon zone

In the street canyon zone, the wind factors are defined according to Eq. B7 where $H < z < H_{sc}$ and $z < H_c$ (adapted from Kaplan and Dinar (1996) and Singh et al. (2008)).

$$\begin{cases} \frac{U_0(D_y)}{V_p(H_{UB})} = sin(2 \cdot \Theta) \cdot [0.5 + \frac{D_y \cdot (D_{os} - D_y}{0.5 \cdot D_{os}^2}] \\ \frac{V_0(D_y)}{V_p(H_{UB})} = sin^2\Theta - cos^2\Theta \cdot \frac{D_y \cdot (D_{os} - D_y)}{0.25 \cdot D_{os}^2}] \\ \frac{W_0(D_y)}{V_p(H_{UB})} = -|0.5 \cdot (1 - \frac{D_y}{0.5 \cdot D_{os}})| \cdot (1 - \frac{D_{os}}{0.5 \cdot D_{os}}) \end{cases} \quad \text{(B7)}$$

where (cf Fig. B7):

θ angle between wind direction and perpendicular to the downwind building wall

D_y distance along y axis from the upstream building wall

D_{os} distance between the upstream and the downwind buildings of the canyon

H_{UB} the upwind building height

H_{SC} the height of the lowest street canyon building

H_c ellipsoid height at the distance D_y (Eq. B3)

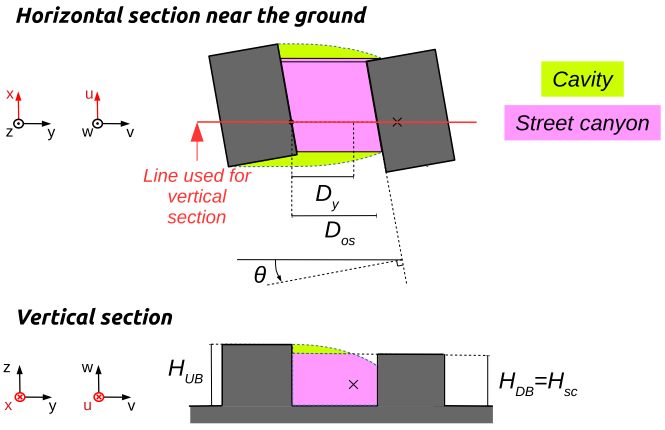

Figure B7. Variables needed for wind factor calculation in street canyon zones

Vegetation in built-up areas

In the *vegetation built* zone, the wind factors are defined according to Eq. B8 where $z < H_{vtm}$ (Nelson et al., 2009).

$$\frac{V_0(z)}{V_p(z)} = \frac{ln(\frac{H_{vtm}}{z_0})}{ln(\frac{z}{z_0})} \cdot exp(\alpha_i \cdot (\frac{z}{H_{vtm}} - 1)) \tag{B8}$$

where (cf Fig. B8):

H_{vtm} the maximum canopy height above the cell of interest

z_0 the roughness length of the surface

z level of the cell

α_i the attenuation factor of vegetation i (=0 if there is no vegetation at height z)

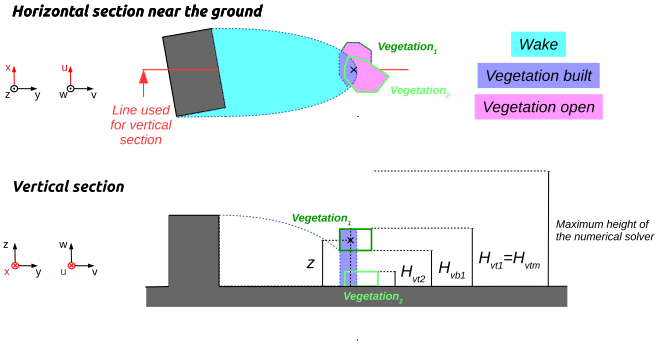

Figure B8. Variables needed for wind factor calculation in vegetation built zones

Vegetation in open areas

In the *vegetation open* zone, the wind factors are defined according to Eq. B9, where $z < H_{vtm}$, and to Eq. B10, where $z \geq H_{vtm}$ (Nelson et al., 2009).

$$\frac{V_0(z)}{V_p(z)} = \frac{ln(\frac{H_{vtm}-d}{z_0})}{ln(\frac{z}{z_0})} \cdot exp(\alpha_i \cdot (\frac{z}{H_{vtm}} - 1)) \tag{B9}$$

$$\frac{V_0(z)}{V_p(z)} = \frac{ln(\frac{z-d}{z_0})}{ln(\frac{z}{z_0})} \tag{B10}$$

where (cf Fig. B9):

H_{vtm} the maximum canopy height above the cell of interest

d is the displacement length (Tab. 1)

z_0 the roughness length of the surface

z level of the cell

α_i the attenuation factor of vegetation i (=0 if there is no vegetation at height z)

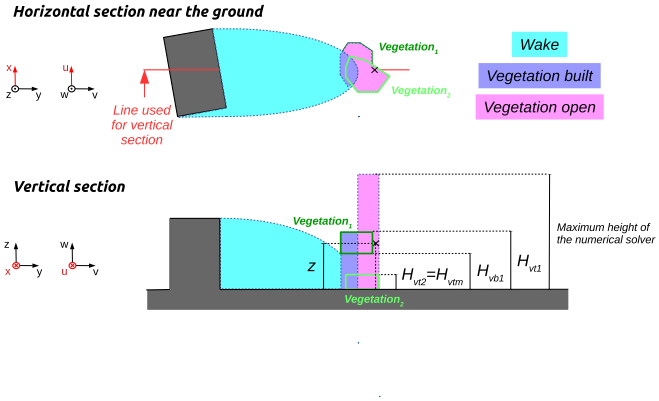

Figure B9. Variables needed for wind factor calculation in vegetation open zones

Author contributions. Conceptualization: JB, FL, SO / Data curation: JB / Formal analysis: JB, FL / Funding acquisition: JB, FL / Investigation: JB, FL / Methodology: JB, FL, SO / Project administration: JB / Resources: JB, FL, SO / Software: JB, FL, SO / Supervision: JB, FL / Validation: JB, FL, SO / Visualization: JB / Writing - original draft preparation: JB / Writing - review and editing: JB, FL, SO

Competing interests. The authors declare that they have no conflict of interest.

Acknowledgements. This project has received funding from the European Union's Horizon 2020 research and innovation programme under the Marie Skłodowska-Curie grant agreement No 896069.

We would like to thank the Architectural Institute of Japan for the data availability of their wind tunnel experiments. ~~Thank you~~ Our gratitude goes to Yoshihide Tominaga for his answers concerning the datasets. We would also like to thank the Los Alamos laboratory to allow us ~~freely using~~ to freely use the QUIC-URB software. ~~Thank you to~~ We would also like to express our thanks to Michael Brown for his help and answers to our questions related to this model. We would also like to thank the reviewer Csilla Gal who reviewed this manuscript and adressed numerous propositions to improve the readability of our text.

References

Bagal, N., Pardyjak, E., and Brown, M.: Improved upwind cavity parameterization for a fast response urban wind model, in: 84th Annual AMS Meeting. Seattle, WA, 2004.

Bocher, E., Petit, G., Fortin, N., and Palominos, S.: H2GIS a spatial database to feed urban climate issues, in: 9th International Conference on Urban Climate (ICUC9), 2015.

Bozorgmehr, B., Willemsen, P., Gibbs, J. A., Stoll, R., Kim, J.-J., and Pardyjak, E. R.: Utilizing dynamic parallelism in CUDA to accelerate a 3D red-black successive over relaxation wind-field solver, Environ. Modell. Softw., 137, 104 958, https://doi.org/https://doi.org/10.1016/j.envsoft.2021.104958, 2021.

Brown, M. J., Gowardhan, A., Nelson, M., Williams, M., and Pardyjak, E. R.: Evaluation of the QUIC wind and dispersion models using the Joint Urban 2003 field experiment dataset, in: AMS 8th Symp. Urban Env, 2009a.

Brown, M. J., Gowardhan, A., and Pardyjak, E. R.: Evaluation of a fast-response pressure solver for a variety of building shapes and layouts, 2009b.

Brown, M. J., Gowardhan, A. A., Nelson, M. A., Williams, M. D., and Pardyjak, E. R.: QUIC transport and dispersion modelling of two releases from the Joint Urban 2003 field experiment, Int. J. Environ. Pollut., 52, 263–287, https://doi.org/http://dx.doi.org/10.1504/IJEP.2013.058458, 2013.

Bruse, M.: ENVI-met 3.0: updated model overview, University of Bochum. Retrieved from: www. envi-met. com, 2004.

Calzolari, G. and Liu, W.: Deep learning to replace, improve, or aid CFD analysis in built environment applications: A review, Build. Environ., 206, 108 315, https://doi.org/http://dx.doi.org/10.1016/j.buildenv.2021.108315, 2021.

Cionco, R. M.: A wind-profile index for canopy flow, Bound.-Lay. Meteorol., 3, 255–263, https://doi.org/http://dx.doi.org/10.1007/BF02033923, 1972.

Fröhlich, D.: Development of a microscale model for the thermal environment in complex areas, Ph.D. thesis, Dissertation, Albert-Ludwigs-Universität Freiburg, 2016, 2016.

Fröhlich, D. and Matzarakis, A.: Spatial estimation of thermal indices in urban areas—basics of the SkyHelios model, Atmosphere-Basel, 9, 209, https://doi.org/http://dx.doi.org/10.3390/atmos9060209, 2018.

Girard, P., Nadeau, D. F., Pardyjak, E. R., Overby, M., Willemsen, P., Stoll, R., Bailey, B. N., and Parlange, M. B.: Evaluation of the QUIC-URB wind solver and QESRadiant radiation-transfer model using a dense array of urban meteorological observations, Urban climate, 24, 657–674, https://doi.org/http://dx.doi.org/10.1016/j.uclim.2017.08.006, 2018.

Hanna, S. and Britter, R.: Wind flow and vapor cloud dispersion at industrial sites. Am. Inst, Chem. Eng-New York, https://doi.org/http://dx.doi.org/10.1002/9780470935613, 2002.

Huttner, S. and Bruse, M.: Numerical modeling of the urban climate–a preview on ENVI-met 4.0, in: 7th international conference on urban climate ICUC-7, Yokohama, Japan, vol. 29, 2009.

Johansson, L., Onomura, S., Lindberg, F., and Seaquist, J.: Towards the modelling of pedestrian wind speed using high-resolution digital surface models and statistical methods, Theor. Appl. climatol., 124, 189–203, https://doi.org/http://dx.doi.org/10.1007/s00704-015-1405-2, 2016.

Kaplan, H. and Dinar, N.: A Lagrangian dispersion model for calculating concentration distribution within a built-up domain, Atmos. Environ., 30, 4197–4207, https://doi.org/http://dx.doi.org/10.1016/1352-2310(96)00144-6, 1996.

Kastner, P. and Dogan, T.: Eddy3D: A toolkit for decoupled outdoor thermal comfort simulations in urban areas, Build. Environ., 212, 108 639, https://doi.org/http://dx.doi.org/10.1016/j.buildenv.2021.108639, 2022.

Li, R., Zeng, F., Zhao, Y., Wu, Y., Niu, J., Wang, L. L., Gao, N., and Shi, X.: CFD simulations of the tree effect on the outdoor microclimate by coupling the canopy energy balance model, Build. Environ., p. 109995, https://doi.org/http://dx.doi.org/10.1016/j.buildenv.2023.109995, 2023.

Lindberg, F., Grimmond, C. S. B., Gabey, A., Huang, B., Kent, C. W., Sun, T., Theeuwes, N. E., Järvi, L., Ward, H. C., Capel-Timms, I., et al.: Urban Multi-scale Environmental Predictor (UMEP): An integrated tool for city-based climate services, Environ. Modell. Softw., 99, 70–87, https://doi.org/http://dx.doi.org/10.1016/j.envsoft.2017.09.020, 2018.

Macdonald, R.: Modelling the mean velocity profile in the urban canopy layer, Bound.-Lay. Meteorol., 97, 25–45, https://doi.org/http://dx.doi.org/10.1023/A:1002785830512, 2000.

Margairaz, F., Eshagh, H., Hayati, A. N., Pardyjak, E. R., and Stoll, R.: Development and evaluation of an isolated-tree flow model for neutral-stability conditions, Urban Climate, 42, 101 083, https://doi.org/https://doi.org/10.1016/j.uclim.2022.101083, 2022.

Maronga, B., Banzhaf, S., Burmeister, C., Esch, T., Forkel, R., Fröhlich, D., Fuka, V., Gehrke, K. F., Geletič, J., Giersch, S., et al.: Overview of the PALM model system 6.0, Geosci. Model Dev., 13, 1335–1372, https://doi.org/http://dx.doi.org/10.5194/gmd-13-1335-2020, 2020.

Matzarakis, A. and Endler, C.: Physiologically equivalent temperature and climate change in Freiburg, 2009.

Matzarakis, A., Gangwisch, M., and Fröhlich, D.: RayMan and SkyHelios Model, in: Urban Microclimate Modelling for Comfort and Energy Studies, pp. 339–361, Springer, 2021.

MENG, Y. and HIBI, K.: Turbulent measurments of the flow field around a high-rise building, Wind Engineers, JAWE, 1998, 55–64, https://doi.org/http://dx.doi.org/10.5359/jawe.1998.76_55, 1998.

Morille, B., Lauzet, N., and Musy, M.: SOLENE-microclimate: a tool to evaluate envelopes efficiency on energy consumption at district scale., Enrgy Proced., 78, 1165–1170, https://doi.org/http://dx.doi.org/10.1016/j.egypro.2015.11.088, 2015.

Musy, M., Azam, M.-H., Guernouti, S., Morille, B., and Rodler, A.: The SOLENE-Microclimat Model: Potentiality for Comfort and Energy Studies, in: Urban Microclimate Modelling for Comfort and Energy Studies, pp. 265–291, Springer, https://doi.org/http://dx.doi.org/10.1007/978-3-030-65421-4_13, 2021.

Nelson, M., Addepalli, B., Hornsby, F., Gowardhan, A., Pardyjak, E., and Brown, M.: 5.2 Improvements to a Fast-Response Urban Wind Model, 2008.

Nelson, M. A., Williams, M. D., Zajic, D., Brown, M. J., and Pardyjak, E. R.: Evaluation of an urban vegetative canopy scheme and impact on plume dispersion, Tech. rep., Los Alamos National Lab.(LANL), Los Alamos, NM (United States), 2009.

Pardyjak, E. R. and Brown, M.: QUIC-URB v. 1.1: Theory and User's Guide, Los Alamos National Laboratory, Los Alamos, NM, 2003.

Pol, S., Bagal, N., Singh, B., Brown, M., and Pardyjak, E.: Implementation of a rooftop recirculation parameterization into the quic fast response urban wind model, 2006.

Ratto, C., Festa, R., Romeo, C., Frumento, O., and Galluzzi, M.: Mass-consistent models for wind fields over complex terrain: the state of the art, Environ. Softw., 9, 247–268, https://doi.org/http://dx.doi.org/10.1016/0266-9838(94)90023-X, 1994.

Robinson, D., Brambilla, S., Brown, M. J., Conry, P., Quaife, B., and Linn, R. R.: QUIC-URB and QUIC-fire extension to complex terrain: Development of a terrain-following coordinate system, Environ. Modell. Softw., 159, 105 579, https://doi.org/http://dx.doi.org/10.1016/j.envsoft.2022.105579, 2023.

Röckle, R.: Bestimmung der Strömungsverhältnisse im Bereich komplexer Bebauungsstrukturen, Ph.D. thesis, 1990.

Sherman, C. A.: A mass-consistent model for wind fields over complex terrain, J. Appl. Meteorol. Clim., 17, 312–319, 1978.

Singh, B., Hansen, B. S., Brown, M. J., and Pardyjak, E. R.: Evaluation of the QUIC-URB fast response urban wind model for a cubical building array and wide building street canyon, Environ. Fluid Mech., 8, 281–312, https://doi.org/http://dx.doi.org/10.1007/s10652-008-9084-5, 2008.

Tominaga, Y., Yoshie, R., Mochida, A., Kataoka, H., Harimoto, K., and Nozu, T.: Cross comparisons of CFD prediction for wind environment at pedestrian level around buildings, Part, 2, 2661–2670, 2005.

Tominaga, Y., Mochida, A., Yoshie, R., Kataoka, H., Nozu, T., Yoshikawa, M., and Shirasawa, T.: AIJ guidelines for practical applications of CFD to pedestrian wind environment around buildings, J. Wind Eng. Ind. Aerod., 96, 1749–1761, https://doi.org/http://dx.doi.org/10.1016/j.jweia.2008.02.058, 2008.

Wellens, A., Moussiopoulous, N., and Sahm, P.: Comparison of a diagnostic model and the MEMO prognostic model to calculate wind fields in Mexico City, WIT Trans. Ecol. Envir., 3, 1970.